THESIS

MAHMUDA RAHMAN

MSc Environmental Engineering

Gödöllő

2023

Hungarian University of Agriculture and Life Sciences

Szent István Campus

MSc Environmental Engineering

DETERMINATION OF SOIL PROPERTIES BY COLOR MEASURING

Primary Supervisor: Dr. András Barczi

Author: Mahmuda Rahman VELW28

Institute of Agricultural and Food Economics

Gödöllő

2023

ABSTRACT

The utilization of soil color as a means of categorizing soil and identifying its characteristics is a widespread technique. Soil moisture, defined as the quantity of water contained within the soil, is a fundamental characteristic of soil that plays a vital role in both the hydrological cycle and plant development. The objective of this study is to establish the correlation between soil moisture and color across various saturation levels, as well as to evaluate the reliability of low-cost colorimeters in the measurement of soil color. A total of 15 sets of soil samples were examined, resulting in the generation of a thorough dataset consisting of 375 color scans conducted using the Nix color sensor. The present study aimed to examine the influence of varying water content on soil by employing the CIELAB color space to assess changes across several saturation phases. The method under consideration has the potential to be utilized for the calibration of discrepancies in soil color acquired by digital scans. Consequently, this would enable a more uniform, unbiased, and precise categorization and assessment of soil samples exhibiting various degrees of moisture content.

Keywords: Soil Moisture, Irrigation, CIELAB, Nix color sensor.

TABLE OF CONTENTS

ABBREVIATIONS AND DEFINITIONS

SDI	Stress Day Index
NCS	Normalized Crop Susceptibility
ET	Evapotranspiration
WSN	Wireless Sensor Network
ML	Machine Learning
AI	Artificial Intelligence
UAV	Unmanned Aerial Vehicles
IoT	Internet of Things
ADC	Analog-to-Digital Converter
GIS	Geographic Information System
RS	Remote Sensing
FDC	Flow Duration Curve
EDOSIM	Evaluation, Design, and Optimization of Irrigational Model
SCE	Shuffled Complex Evolution
DI	Drip Irrigation
SSDI	Subsurface Drip Irrigation
ADI	Alternating Drip Irrigation
MDI	Mulched Drip Irrigation
EWP	Economic Water Productivity
LPL	Land Productivity Level
WP	Production Efficiency
NPK	Nitrogen, Phosphorus, and Potassium
MP	Microplastics
SOC	Soil Organic Carbon
TN	Total Nitrogen
SQI	Soil Quality Index
VRA	Variable Rate Application
OM	Organic Matter
RGB	Red Green Blue
GLCM	Gray-level Occurrence Matrix
SVM	Support Vector Machine
CNN	Convolutional Neural Network
LBP	Local Binary Pattern
WRB	World Reference Base
USDA	United States Department of Agriculture
SAD	Spectral Analysis Device
NDVI	Normalize Difference Vegetation Index
XRD	X-Ray Diffraction
RSISC	Remote Sensing Image Scene Classification
HSV	Hue Saturation Value
TSC	Two-Layer Sparse Coding

DBF	Deep Belief Network
FACNN	Feature Aggregation Convolutional Neural Network
LSE-Net	Local Semantic Network
AGOS	All Grains One Schema
HCS	Hybrid Color Space
AHCS	Adaptive Hybrid Color Space
MSCC	Munsell Soil Color Chart
CIE	Commission Internationale de l´Eclairage
LED	Light Emitting Diode
CMYK	Cyan-Magenta-Yellow-Black

ACKNOWLEDGEMENTS

I would like to sincerely appreciate my supervisor, Dr. András Barczi, for the continuous and unrelentless support that he has accorded me during my research period. He has offered his guidance and experience which has been of great help through the challenges encountered during the research.

The Hungarian University of Agriculture and Life Sciences teaching and non-teaching fraternity has been very instrumental in imparting me with knowledge related to my studies and providing the best environment for one to excel in their studies. It has really been an honor being part of this amazing community to which I am really grateful to.

Many thanks to the Thesis Review Team whose encouragement and support have ensured the successful completion of this thesis.

Finally, I would want to thank my family for being very understanding and supportive throughout my study period. Their constant encouragement has been very reassuring and has given me the very much required zeal to successfully complete my research.

Thank you to all!

LIST OF FIGURES

LIST OF TABLES

1. INTRODUCTION

The quantity of water contained below the active layer of soil is commonly known as "soil moisture". The uppermost layer of the soil profile, commonly located within the first to second meter, is typically referred to as this active layer. The significance of this matter cannot be exaggerated, since it functions as the primary source of water for both agricultural activities and the maintenance of indigenous flora. One crucial consideration is the extent to which soil moisture in the shallow subsurface impacts the allocation of surface energy between sensible and latent heat exchange with the atmosphere. The establishment of a link between the water and energy balances is facilitated by the temperature and moisture content of the soil. The moisture present in the soil plays a crucial role as the major reservoir of water that is lost through evaporation and transpiration from both the soil and vegetation. Consequently, it exerts an influence on spatial patterns that govern the development of clouds and precipitation. The regulation of surface temperature is influenced by the quantity of soil moisture, with a general trend indicating that higher levels of soil moisture correspond to lower surface temperatures. This phenomenon can be ascribed to the fact that evapotranspiration, which encompasses both transpiration and evaporation, consumes a greater proportion of the total available energy compared to surface heating. Consequently, there is a decrease in the surface temperature. The phenomenon of runoff, which ultimately determines the quantity of precipitation or snowmelt that directly flows into rivers and streams and, in severe circumstances, contributes to the occurrence of flooding events, is significantly impacted by the moisture content of the soil. There exists a significant correlation between drought and diminished levels of soil moisture, and the interplay between soil moisture and the atmosphere plays a vital role in the endurance of drought conditions. As a result of this phenomenon, soil moisture, which refers to the amount of water present in the soil, assumes a critical function in both the hydrological cycle and the growth of plants.

Irrigation refers to the regulated practice of supplying water to the soil in order to sustain optimal soil moisture levels, hence creating suitable conditions for robust plant growth during the cultivation period. Optimal soil moisture levels are necessary to create a conducive environment for plant growth. In order to maintain constant annual yields, full-season agronomic or high-value specialty crops are frequently subjected to irrigation throughout the growing season. The consideration of soil-water compatibility is a key element in the context of irrigation. The utilization of irrigation water in the presence of incompatibility has the potential to exert adverse effects on the chemical and physical properties of the soil. The factors mentioned above may have a detrimental impact on plant growth. In order to determine the suitability of a parcel of land for irrigation, a comprehensive analysis of the soil's characteristics, the topography of the field, and the quality of water planned for irrigation is necessary. Gaining comprehension of the optimal quantity and timing of water allocation is a fundamental aspect of effective management. The aforementioned phenomenon exerts a substantial impact on the moisture content of the soil, a critical factor in preserving the soil's inherent characteristics.

Due to their high cost and time constraints, traditional wet chemistry-based soil characterization systems are not as capable of providing immediate soil information. Despite the methods' broad use and precision, this issue still exists. Furthermore, it should be noted that there may be significant discrepancies in the lab results due to the use of inaccurate point sampling techniques and the failure to observe minute interactions between the different components of the soil. This issue frequently leads to a decline in the accuracy of the interpretation of soil test results. This study aims to determine the link between soil moisture and color at different saturation levels and to test the accuracy of inexpensive colorimeters in assessing soil color. The Nix color sensor, which makes use of the CIELAB color space, was used to examine the possible association between the moisture content of ground surface soil samples and their color properties. In order to conduct the study, soil samples were analyzed at five different saturation levels, ranging from high saturation to low saturation. The aim of the study was to ascertain the relationship between the soil's color and water content. There were five repetitions in all of the experiment's repetitive conduct. 15 batches of soil samples were analyzed and a comprehensive dataset comprising of 375 color scans utilizing the Nix color sensor was produced. The impact of changing water content on soil properties was investigated using the CIELAB color space to look at changes in different saturation phases. The color parameters (L*, a*, and b*) acquired using the Nix Pro apparatus were selected for examination because, in comparison to other parameters, they were shown to have a higher correlation with one another at different phases. The post-harvest phase was when the soil samples were collected from a cereal field.

This is how the remaining content of the paper is structured. The literature review is discussed in Section 2, and the methodology, including the color analysis, location, and soil sample, are covered in Section 3. The statistical analysis is explained in Section 4, and the result is presented in Section 5. Section 6 provides a conclusion.

2. LITERATURE REVIEW

This section will go into the description of different irrigation methods and its impact on soil characteristics, various soil types, remote sensing techniques, and different colorimeters and color space used for the analysis of soil properties. The information presented in this area is derived from a recent literature survey of scholarly publications and articles. The analysis of soil color using various approaches has been extensively investigated by numerous researchers, with a significant historical background.

2.1 Irrigation

Irrigation is a key agricultural practice that involves the artificial application of water to soil in order to stimulate crop and plant growth. The goal of irrigation is to make the soil more conducive to crop and vegetation growth. Because it offers a reliable and regulated water source for crops, it is vital in today's agricultural practices because it allows farmers to compensate for little rainfall and ensure that plants continue to develop normally (Chen et al., 2021b). Throughout human history, irrigation has been the essential component of human civilization. Ancient communities in Mesopotamia, Egypt, and the Indus Valley all made use of irrigation systems in order to foster the growth of agriculture, their people, and their societies (Harmanny and Malek, 2019).

It is impossible to overstate the importance of irrigation to contemporary farming practices. It ensures a consistent flow of water to plants, which promotes healthy growth and ultimately leads to improved crop yields, which in turn supports the expansion of agricultural production. In addition to this, it is an essential approach for reducing risks, as it lessens the impact of extreme weather events like droughts and unpredictable rainfall, which in turn reduces the possibility of a crop failing. Irrigation also broadens the range of plant species that may be grown in a diverse range of temperatures and geographical locations, which ultimately leads to an increase in the amount of food that can be produced from agriculture. In addition, it is essential to the provision of a stable food supply in order to meet the requirements of a growing worldwide population. This is because of the importance of global food security. The water source (rivers, lakes, wells, or reservoirs), the distribution system (pipelines, canals, or pumps), the control system (which may be manual or automated with timers and sensors), and the irrigation equipment (which, depending on the method, may include pumps, valves, hoses, and delivery systems) are all important components of irrigation systems. In order to reduce the amount of water that is wasted and the amount of harm that is done to the environment, it is vital to have irrigation practices that are both effective and sustainable. Excessive irrigation can lead to a variety of issues, including waterlogging and the salinization of the ground. Modern technologies like as drip and sprinkler systems have been developed with the intention of reducing overall water consumption while simultaneously improving water efficiency.

A great deal of progress has been made in the field of irrigation systems throughout the course of time. Between the years 1970 and 1985, researchers were interested in finding ways to optimize irrigation as a result of the development of more complex monitoring systems and constraints placed on the amount of water that could be used for irrigation (Gamal et al., 2023). In the late 1970s, as a result of population growth and the depletion of natural resources, there was a rise in the demand for water, which led to the development of intelligent irrigation systems that use building layers to boost consumption efficiency and information. In light of the circumstances, it was necessary to develop new approaches to irrigation. It is common information that in order to achieve irrigation optimization, one must take into account the stress day index (SDI), elements of normalized crop susceptibility (NCS), evapotranspiration (ET) crop canopy, and climatic variables (Yang et al., 2021). After the Internet became widely accessible in 1989, new control systems and data storage methods were developed that were based on the internet. These new methods were implemented on the web. Since the year 2000 (Gunther Wyszecki and Stiles, 2000) wireless sensor networks (WSN) have been steadily climbing the ranks of preferred methods for environmental monitoring thanks to their low cost and high degree of dependability. Actuators and sensors are used in a wide variety of WSN applications, including those used in agriculture. WSNs increase the value of preexisting irrigation systems by providing farmers with up-to-the-minute information on the amount of water their crops require to thrive. In addition, provide wireless sensor networks (WSNs) with efficient routing protocols that can monitor and manage irrigation water applications using a variety of different methods. Researchers in the field of precision agriculture have been paying close attention to innovative applications and strategies for irrigation, soil fertilization, insect management, and disease forecasting (Lakhwani et al., 2018). These applications and strategies make use of cutting-edge advanced technologies such as machine learning (ML), artificial intelligence (AI), unmanned aerial vehicles (UAV), and the internet of things (IoT). Farmers nowadays are facing a variety of challenges in the agricultural industry, including those pertaining to the fertility of the soil and the irrigation of plants. Both changes in temperature and rainfall patterns have been highly unpredictable throughout the course of the last few decades. Because of increased food demand as well as population expansion, there may be an increase in the amount of water used in agriculture. Irrigation already accounts for 80 percent of the total water used in agriculture. The administration of water is yet another important problem facing the earth. It is of the utmost importance to optimize the use of water, fertilizers, and human resources in order to achieve the greatest potential agricultural output with the fewest possible expenses. A low-cost autonomous irrigation system that is based on Arduino and uses a soil moisture sensor in (Mahmud and Nafi, 2020) as a way to develop and carry out an inventive idea for farming applications. This system would be used to monitor the moisture content of the soil. The device makes use of an Arduino-UNO, which contains an ADC (Analog-to-Digital) converter on the circuit board. The output of the soil moisture sensor is determined by the state of the soil. Real-time updates to irrigation schedules have the goal of increasing crop yields and reducing the amount of water stress that crops experience. This is accomplished through the management of soil moisture. For evapotranspiration (ET), commonly known as evaporation and transpiration, plants require water. Nevertheless, an excessive amount of water might be detrimental to the health of some plants. When calculating the amount of water that a plant needs, the stage of its growth, the environment, and the type of crop are all taken into consideration. As a result, we are going to be planning irrigation systems that are more efficient with water. Find out how the various strategies of irrigation scheduling effect maize yield and water productivity in arid sandy soils, and then provide irrigation scheduling suggestions that maximize marginal profit per unit of water that is used.

It is possible to collect water from a wide number of water sources and use that water for a wide variety of irrigation methods. The ultimate purpose is to ensure that each plant receives the appropriate amount of water by evenly distributing water across the entire area. The modern irrigation techniques that are used today are designed to provide water specifically to the plant's root zone or crop. The use of modern techniques allows for a significant reduction in water waste, an equitable distribution of the supplied water and energy savings, and an effective control of the irrigation phase.

For instance, it is anticipated that the surface irrigation system will supply the root zone reservoir in a manner that is both uniform and efficient in order to alleviate the stress that is placed on the plant and to encourage the conservation of resources such as water, nutrients, energy, and labor. The irrigation system can also be utilized to either warm the environment in order to prevent plants from frost damage in colder climates or cool the environment in order to protect certain sensitive fruits and vegetables from being exposed to excessive heat. In addition to this, the salts that are developing in the root zone need to be leached out via an irrigation system. In addition to this, it might be utilized to disperse insecticides, add fertilizer to the area, or loosen the soil in order to improve agricultural practices. Surface irrigation is a method of irrigation that is frequently used due to the fact that it is both straightforward and efficient in its water and power consumption. This makes surface irrigation one of the most common and widely used methods of irrigation. Despite the fact that deep percolation and uneven distribution of irrigation water are most commonly associated with inefficient irrigation application efficiency, a number of research have attempted to address this problem in order to increase the efficiency of surface irrigation. Evaluation of Long-Term Resource Factors Produced by Irrigated Agricultural Land Long-term resource factors produced by irrigated agricultural land include soil level, soil drains, and soil texture (Worqlul et al., 2019). Other physical soil qualities are land ramp, land usage, and closeness to water sources to evaluate eligible sites for irrigation purposes on a small, medium, and large scale; and to evaluate acceptable surface irrigation land. Both of these goals were intended to be accomplished by the research presented in (Muluneh, Tadesse and Girma, 2022). An Analytic Hierarchy Process, which incorporated a Geographic Information System (GIS) based multi-criterion evaluation, was utilized in order to determine whether or not the land could support irrigation systems. The suitability of irrigation land was broken down into four categories: highly appropriate (S1), moderately acceptable (S2), marginally appropriate (S3), and currently not appropriate (N). Using Remote Sensing (RS) and Geographic Information System (GIS) methodology, an evaluation of the availability of land surface water in the Gilgel Gibe watershed and its feasibility for use in surface irrigation was carried out in (Akalu, 2022). In order to estimate the availability of surface water, a flow duration curve (FDC) was first calculated, and then the 90% available flow of the Gilgel Gibe River was analyzed. The appropriateness of the land surface was determined by employing a method called MCE, which took into account the communication between important land suitability criteria such slope, soil type, proximity to rivers, and land usage. This irrigation-based approach (Akbari et al., 2018) determined the amount of water that had entered the soil without obtaining advanced or recession data. It did this by determining how much water had reached the soil. The primary purpose of this work was to design, develop, and validate an Evaluation, Design, and Optimization of Irrigational Model (EDOSIM), such as a surface irrigation model of simulation optimization. The simulation was used to test the accuracy of the quantity estimate, and it entailed constructing or evaluating basin, furrow, and border irrigation. Twenty different meta-heuristic procedures were used in an effort to improve the results. When the simulated results of the EDOSIM approach were compared to those of the SIRMOD software's Hydrodynamic technique, both the suggested method for estimating the volume of infiltration and the EDOSIM model performed very well, with CRM = 0.005, NRMSE = 4.2%, RMSE = 0.068, and R2 = 0.988. These values indicate that the proposed method and the EDOSIM model are accurate (Akbari et al., 2018). In addition, it was shown that the strategy known as Shuffled Complex Evolution (SCE) is the most effective way to improve field performance; the target function was decreased in all of the fields. One study (Pramanik et al., 2022) found that surface irrigation had an effectiveness of 86.6% when compared to subsurface irrigation. Built and tested in a layout of a level basin with a fixed end in sandy loams soil was a wireless link between the soil moisture sensors and an automatic checkpoint that can be remotely operated using data from real-time soil moisture conditions. This link was put through its paces in a scenario where it was required to use data from real-time soil moisture conditions. Within the framework of the design of the basin, an effort was made to position the sensor in the most optimal possible spot in order to maximize the efficiency of the irrigation system. In order to control the volume of water passing through the concentration of the water supply system, an automatic check gate made of aluminum and supported by a steel structure was constructed. At a depth of 37.5 centimeters, 15 centimeters, and 7.5 centimeters, respectively, and at 25%, 50%, and 75% of the field's length, three capacitance-based soil moisture sensors were placed (Pramanik et al., 2022). According to the positions of the soil moisture sensors, there are three distinct operating schedules that come into play when there is a 40%, 30%, or 20% deficit in the amount of soil moisture. According to the findings of the study (Pramanik et al., 2022), sensors ought to be set up in locations where there is a soil shortage combined with increased moisture at a depth of 37.5 centimeters and a distance of 25% from the injector. When there is a shortage of moisture, the sensors should be positioned so that they are 7.5 centimeters deep and 75% of the way away from the entry (Pramanik et al., 2022).

Irrigation via drip is an important strategy that can be utilized in the fight against the global water shortage. Drip irrigation is also known by its alternate name, trickle irrigation. The method of watering a plant that is known as "drip irrigation" works by gradually delivering a small amount of liquid to the plant's roots. Because it reduces the quantity of water lost to runoff and evaporation, this kind of irrigation might be the most efficient. Drip irrigation is utilized extensively in modern agriculture, and it is commonly combined with organic or inorganic (plastic) mulches. This is due to the fact that these combinations bring additional benefits, such as less evaporation, enhanced soil temperature, weed control, and so on. However, the problem of drip irrigation emitter blockage has a substantial negative affect on irrigation efficiency and uniformity, and it can even render the system inoperable while simultaneously reducing crop output (Shi et al., 2022). This study (Barkunan, Bhanumathi and Sethuram, 2019) presents an automated drip irrigation system for use in agricultural settings. The technology is put through its paces in a paddy field for a period of three months. According to the experimental setting, it conserves approximately 41.5% of the water that is used by traditional flood irrigation systems and 13% of the water that is used by drip irrigation systems. This study (Wang et al., 2022) illustrates how the three different types of drip irrigation—surface drip irrigation (DI), subsurface drip irrigation (SDI), and alternating drip irrigation (ADI)—affect the yield of tomatoes and the microbial reactivity of the soil. It was found that the homogeneity of moisture distribution in the soil in the root region (zero to sixty centimeters depth) was lowered according to the order SDI > DI > ADI. The tomato root lengths that were created by the SDI method were 4.83 and 3.94 times longer than those that were produced by the ADI and DI methods, respectively. The 1.23 times longer roots that were present in the ADI treatment in comparison to the DI treatment led to a variety of different microbial interactions between the roots and the soil. The SDI treatment produced the most beneficial root-soil-microbe interactions, followed by the ADI treatment and then the DI treatment. Variations in the root-soil-microbe interactions have an effect on the amount of tobacco produced. When compared to the DI and ADI approaches, the SDI method produced results that were 9.77% and 7.77% more favorable than those obtained from the tomato field. The ADI method resulted in a tomato yield that was 24.09 percentage points higher than the DI method. As a consequence of this, various ways for watering tomatoes with drip irrigation can influence the root-soil-microbe interactions that govern tomato production. The findings of this study can be put to use to improve the capacity of drip irrigation systems to control the microbial interactions that occur between plant roots and soil, so leading to an increase in tomato production. The traditional irrigation methods are substantially more water-intensive than the modern drip irrigation technology, which consumes significantly less water. In addition, different types of crops, such as paddy, have varying water requirements during the growth process. According to (Zong et al., 2023), the use of MDI (mulched drip irrigation) on a long-term basis will result in an improvement in the condition of the soil. The findings illustrate MDI's long-term impact on soil quality and supply valuable information that can be used to evaluate the practicability of MDI application within the context of a manmade oasis over the long term. In order to generate an exhaustive soil quality index, this study made extensive use of a variety of data set approaches. In this study, important indicators of soil quality, such as bulk density, three-phase ratio, stable mechanical aggregate, water-stable aggregate, soil salinity, pH, total nitrogen, total carbon, organic carbon, available phosphorus, microbial biomass carbon, microbial activity, cellulase activity, phosphatase activity, and soil microbial diversity, were each described in detail. Cotton production efficiency (WP), economic water productivity (EWP), and land productivity levels (LEP) were analyzed in this study (Çetin and Kara, 2019) using a variety of irrigation water rates and drip irrigation techniques (SDI and subsurface drip irrigation (SSDI)). The results of an experiment that was conducted over both the 2016 and 2017 cotton growing seasons were evaluated. SSDI was able to lower the amount of water that was required while simultaneously increasing the productivity of water by using an irrigation water quantity that was based on the plant's water needs. The application of this technology to agricultural practices was consequently enhanced. In conclusion, in order to optimize water production and conserve water for irrigation methods and farmers, it is essential to take into consideration WPIng, EWP, WP, and LEP. In this study (Wang et al., 2021), which utilized pear to view two years' worth of irrigation research, the two components of drip irrigation system pipe design and soil moisture lower rate were taken into mind. Five different drip irrigation modes and management strategies were utilized in this study in order to investigate the impact that drip irrigation methods have on the water production of the field and to enhance the effective utilization of available water resources. After taking everything into consideration, it was found that the SSDI with two points below a soil moisture lower level of 60% FC was the most effective irrigation method for a pear crop. This was the conclusion reached after all factors were considered.

Irrigation via sprinklers is accomplished by blasting water into the air, where it eventually condenses into precipitation. The spray production is controlled by the pressure of the water, which in turn is controlled by a system consisting of pipes and very small nozzles. It is essential to make an informed decision on the sprinkler layout and the operating pressure when selecting the nozzle diameters. Depending on the pace at which the soil loses water, the quantity of water that must be used to irrigate crops and replace the root region can be used practically uniformly at a rate that is deemed acceptable (Goap et al., 2018). The spray irrigation system enables the cultivation of a wide variety of crops, including vegetables such as onions, potatoes, carrots, and lettuce as well as other types, as well as spices such as cardamom and pepper, flowers such as jasmine and carnations, oilseeds such as sunflower, groundnut, and safflower, and fibers such as cotton and sisal (Bortolini and Tolomio, 2019). Sprinkler irrigation is adaptable to a wide variety of soil compositions, with the notable exception of compacted clay. Additionally, it allows for greater movement in the system and helps to preserve water. It is ideal for oilseeds and vegetables, and it is appropriate for irrigating plants in situations where there is a high plant population in relation to the available land area. Sprinkler irrigation systems can be completely portable, slightly portable, semi-permanent, or completely permanent, depending on the degree to which they can be moved about. These categories are based on the degree to which they can be moved. By lowering the working pressure of the sprinklers, it is possible to significantly cut down on the amount of energy that is consumed for sprinkler watering. However, the sprinkler's hydraulic performance will invariably vary if the operating pressure is lowered or if the geometry of the nozzle is altered. As a result, experiments were carried out to investigate the relationships between operating pressures, injector shapes, and diameters, as well as flow rate, throw radius, and irrigation. water flow rate, droplet size, and spinning droplet speed sprinklers, in addition to the kinetic energy of water droplets that the topsoil to evaluate the various spray quality sprinklers that aren't circular. water flow rate, droplet size, and spinning droplet speed sprinklers. It was able to compute the watering similarity coefficients for circular and non-circular injectors by altering the operating pressures and spacing of the rectangular sprinklers. Under the identical conditions of operating pressure and nozzle size, the circulation flow rates and non-circular injectors were equal. On the other hand, the throw radius of the circular nozzle was larger than the throw radius of the non-circular nozzle. In addition, the droplets produced by a circular nozzle are significantly larger than those produced by a nozzle that is not round (Chen et al., 2022).

Irrigation has repercussions that are both good and bad for the land. The provision of a consistent and reliable water supply is a benefit offered by irrigation, which can result in a large increase in the output of the crop. Because it ensures that crops will have access to an adequate amount of moisture throughout their entire growth cycle, this is of utmost significance in regions that experience infrequent or scant precipitation. The capacity of irrigation to widen cropping patterns allows for the cultivation of a broader diversity of plant species, some of which may not do particularly well in the climate of the area. The increased food security and financial rewards that can result from this diversification are also possible outcomes. Irrigation can assist provide a consistent supply of food for growing populations, while also mitigating some of the negative effects that come along with prolonged dry spells and inadequate water availability. It also reduces the likelihood of the crop being unsuccessful.

The quantity, diversity, composition, and assembly of communities of soil denitrifies that comprise the nirS, nirK, and nosZ genes were investigated in study (Yu et al., 2023) in soils that had been subjected to long-term (11 years) fertilization and irrigation managements. These soils had also been managed in a manner that included irrigation. The results showed that irrigation significantly increased the abundance of the nirS, nirK, and nosZ genes in the chemical fertilizer (NPK) treatments and in the manure treatments when compared to the control without irrigation. This was in contrast to the situation where there was no irrigation. Regardless of the presence or absence of fertilization, the community assembly of the nirS-type denitrifier was driven from a stochastic process to a deterministic one as a result of irrigation. On the other hand, the nosZ-type was driven from a stochastic process to a deterministic one as a result of irrigation. In this study (Liu et al., 2023), the "MP (microplastics) communities" before and after irrigation in a typical agricultural irrigation area of the Yellow River were examined, along with the distribution of the denitrifiers. This highlights the relevance of irrigation in controlling soil denitrification related microbes, which is highlighted by the fact that irrigation, rather than fertilization, significantly influenced the changes in abundance, community structure, network structure, and assembly process of the denitrifiers. After irrigation, there was an increase in the number of MPs found in surface water and sediment, while there was a decrease in the number of MPs found in the surface soil of the cornfield. The migration of MPs in a vertical direction was sped up by irrigation, which helped them penetrate deeper into the soil. In addition, irrigation weakened the connection between the soil's major components and its qualities. According to the findings, river irrigation raises the level of microplastic pollution in deep soil and generates secondary microplastic pollution in the environment of the soil. Isotopes of strontium, when used as a tracer in the environment, can determine how the physiochemical properties of soil have been altered as a result of urbanization. The chemical and spatial composition of the soils has been dramatically altered as a consequence of urbanization. Because of this, it's possible that soils will no longer be able to provide the ecosystem services that are necessary to maintain the health and resiliency of the environment. A different study (Mauceri and Banner, 2023b) found that metropolitan areas might potentially evaluate and maintain their water infrastructure in a more effective manner to reduce the amount of water that is lost due to leaks and irrigation. Irrigated fields were found to have significantly higher values for the bulk of the analyzed soil properties compared to non-irrigated fields or rain-fed fields, as stated in the conclusions of the experiments presented in . (Yemane Weldewahid et al., 2023) Long-term irrigation increased the amount of SOC (soil organic carbon) and TN (total Nitrogen) stocks in the field by 14.1% and 30%, respectively, in compared to the field that relied solely on rain-fed production. Continual watering practices led to a rise of 40.1% in the soil quality index (SQI). The overall findings of the study imply that transitioning from a rain-fed agriculture approach to an irrigated agriculture method improves soil quality, soil organic carbon stores, and total nitrogen stocks during the course of the study.

However, overwatering the soil for an extended period of time might diminish its capacity to hold moisture. An improper management of the irrigation system might lead to soil infiltration. Salts and minerals are washed away gradually over time as a result of water being absorbed by the soil and then evaporating. It is possible for salty soil to produce an unfavorable environment for plants and to diminish the quantity of moisture that is accessible in the soil. This is caused by the fact that saline soil reduces a plant's ability to absorb water. The phenomenon known as waterlogging takes place when the soil is continually saturated with water. It is a situation that can be brought on by either inefficient irrigation practices or excessive irrigation. This issue reduces the quantity of oxygen that is available to the roots of the plant, which can result in root rot and other issues. Wetlands have the potential to have a negative impact on both the structure of the soil and its capacity to efficiently store precipitation. In this work(Ramos et al., 2023) , the complex ion chemistry module of the HYDRUS-1D model was used to analyze the soil water and salt balance in nine commercial orchards located in Portugal throughout the 2019 and 2020 growth seasons. These orchards were analyzed over the course of two years. The hazard of salinity build-up was medium to very high for the majority of fields during the really dry years. This is because the possibility that salt buildup during this time did not exceed a specific level. The duration of the crop growth phase, the distribution of rainfall throughout the late and non-growing periods, the features of the soil drainage, and the quality of the irrigation water were the factors that controlled the amount of salt that accumulated. The irrigation strategy, seasonal irrigation and rainfall depths, and the length of the crop growth phase were all factors. Sometimes, the kind of soil also plays a role in determining how the effects of irrigation on soil quality manifest.

2.2 Soil Classification

Soil classification is an ever-evolving subject, encompassing everything from the organizational structure of the system to the definitions of the classes to their applications in the field. Both the viewpoint of soil as a material and the viewpoint of soil as a resource are viable ways to approach the classification of soil. Researchers have devised systems for classifying soils based on a wide range of characteristics, including their chemical make-up, physical characteristics, fertility levels, and geographic locations.

The surface texture of the soil has a substantial influence on a number of different qualities, including the type of plant that grows there, its capacity to store water, its permeability, its capacity to hold soil nutrients, its porosity, and its saturated hydraulic conductivity (Xia, Rufty and Shi, 2020). Therefore, it is an essential criterion for the categorization of soil, which can be broadly categorized as sand, loam, and clay, with additional sub-classifications based on the proportion of sand, silt, and clay present in the mixture. Clay soils often contain a high level of organic matter, but they have a low capacity for storing water and poor permeability. Sandier soils, on the other hand, have a reduced capacity to hold onto organic matter and water, while loamy soils have a texture that falls between that of clay and sand (Khairul Huda Yusof et al., 2022). Because the textural properties of soil are so important, they are utilized in precision agriculture for the purpose of managing soil and nutrients in a more targeted manner. The following are the three primary categories into which classification systems for soil texture can be placed: 1) analysis of silt, 2) spectroscopy, and 3) approaches based on images. The traditional method for determining the texture of soil involves doing laboratory sediment analyses. In order to use these procedures, you will need to investigate the size of the soil particles. Pipetting and the Bouyoucos method (also known as the hydrometer method) are two prominent sediment analysis procedures that are used to determine soil texture. These procedures include collecting samples, processing them, treating them, screening them, and drying them. The Bouyoucos method determines the size of soil particles by comparing the starting and ending densities of the soil while it is suspended in an aqueous solution. The texture of the soil can be determined using the pipette method by determining the weight of a soil sample. An investigation of the Bouyoucos method demonstrated that, in order to attain a higher level of precision, the ground must first be pre-treated with hydrogen peroxide and Calgon (Mwendwa, 2022). These procedures require a significant amount of time and effort, as well as being impossible to scale up for use in the real world. In addition, because these processes include the utilization of oxidants that are known to be corrosive, they are not kind to the environment. In addition, the texture mapping in the lab has a low resolution both spatially and temporally and does not support VRA (variable rate application). The classification of soil texture frequently makes use of spectroscopy. The analysis of soil texture is frequently carried out through the use of near-infrared spectroscopy. This determines how effectively certain soil textures absorb different amounts of energy. Memory-based learning and near-infrared soil spectroscopy were both utilized in one study (Jaconi, Vos and Don, 2019) to accurately predict soil texture. Another study looked into this topic in further depth by analyzing the performance of various spectral regions by employing a stereoscopic regression method to make predictions about the soil texture (João Augusto Coblinski et al., 2020b). When there is sufficient data, spectroscopy that is integrated with deep learning performs better than conventional approaches to spectroscopy (Ng et al., 2020). Even if the combination of soil spectroscopy and deep learning produces promising results, this method requires the collecting of soil samples and the preparation of those samples in a laboratory. This takes a lot of time and money, and as a result, we end up with smaller sample sizes that aren't very representative of the overall field. Recent developments in machine learning, data storage, computer vision, and image processing have led to research evaluating the power of photographs in categorizing soil qualities such as organic matter (OM) and texture (Augusto et al., 2020a), (Fan et al., 2017). These studies may be found in a variety of academic journals. Several different image analysis approaches can be helpful in producing trustworthy results for the classification of soil texture. They are able to be sorted into a few distinct categories; the statistical technique makes use of picture characterization through the application of histograms, autocorrelation matrices, and co-occurrence matrices. Grayscale and RGB (red, green, blue) images that were transformed to histograms were used in certain research to classify soil samples taken from a depth of fifty centimeters (Chung et al., 2012). In another piece of research, researchers used something called a gray-level occurrence matrix (GLCM) to categories the various kinds of crops. The GLCM algorithm is responsible for the extraction of features from grayscale images, which are then used for classification using support vector machines (SVMs), random forests, naive Bayes, and neural networks (Iqbal et al., 2021). Grayscale photographs are given a GLCM treatment in order to enhance the features of the images and the information contained in the pixels. After that, statistical features including contrast, correlation, and homogeneity are generated using the GLCM and applied to the K neighbors for the purposes of classification. The high-dimensionality of the matrix is a drawback of the GLCM method, despite the fact that it is an extremely helpful classification tool (Ayushman Ramola, Amit Kumar Shakya and Dai Van Pham, 2020b). Methods of statistical image analysis, such as histograms and GLCM, are utilized in order to improve significant picture pixel characteristics and information, both of which are required for classification. The structural approaches operate under the assumption that picture texture data can be found in a spatial context. Models like the area model, the moment model, the eccentricity model, the elongation model, and the local binary model are some examples. Image categorization can be accomplished by the use of many methods, including moment invariance and deep learning. The classification procedure achieves higher levels of accuracy and sensitivity when image moments are used in conjunction with deep learning. Image moments are a scalar quantity that are used to capture the features of an image based on the spatial distribution of the picture's pixels. picture moments are measured in pixels. In one investigation, the categorization process utilized LBP in addition to mean, median, and most common pixel values. Following the selection of the most useful elements, a machine learning algorithm is applied to the data in order to categories the texture as either sand, silt, or clay (Uddin and Hassan, 2022). The improvement of texture data is accomplished by the use of transformation-based approaches, which rely on picture transformation. The transform of the Fourier series and the wavelets (Gabor) are two examples. In addition to SVM, the Gabor filter and histogram equalization are both utilized in the classification of textures (Shivhare and Cecil, 2021).

The many existing approaches for classifying the texture of the soil rely on photographs of the soil that were captured in controlled environments. These methods are not scalable to highly spatio-temporal soil texture mapping and do not reflect the problems and variations that occur in the real world. This research (Babalola, Asad and Bais, 2023) proposes a novel, scalable, high-spatial-resolution ground surface texture classification procedure. It makes use of image processing, texture enhanced filtering, and convolutional neural networks (CNN) for the purpose of classifying ground images captured under uncontrolled field conditions. The purpose of this research is to overcome the limitations previously mentioned. The suggested method incorporates a number of procedures designed to enhance the soil image analysis. In the beginning, image segmentation is utilized to clean the image of pixels that are irrelevant to the ground and get it ready for future processing. After that, the segmented output is broken into smaller cells to separate relevant background pixels from the rest of the backdrop. After that, a high-frequency filter is applied to the image in order to enhance the texture of the picture. According to the findings of this research, Gabor filters are more useful than local binary patterns (LBP) at accomplishing this goal. By developing four unique Gabor filters, we are able to bring out particular patterns that were previously obscured in the soil image. In the final step, CNN classifiers are trained with the deconstructed and improved images in order to provide the most accurate analysis possible. They assessed the performance of the proposed framework utilizing a variety of measures and compared it to other state-of-the-art soil texture categorization frameworks already in existence.

WRB is an international system for classifying soils that is used to give soils names and to provide legends for soil maps. Both the general public and the scientific community make use of the materials that are offered by FAO-WRB in order to improve their understanding of soil science. In a similar manner, the United States Department of Agriculture (USDA) has also developed soil categorization schemes, which are based on quantitative soil attributes, in order to categories soils in a form that can be easily applied in the field or in the agriculture laboratory. The categorization of land, on the other hand, is frequently done in accordance with spatial allocation for the sake of regional planning and expansion. The spatial distribution of different types of soil or their attributes can be represented by digital soil mapping, which can signify ambiguity in soil forecasts. It also supplied soil-specific interpretations and risk evaluations, as well as produced the first soil study maps, modified or modernized existing surveys, and constructed the first soil study maps. Input data might come from either historically recorded soil maps or spectral information acquired using remote sensing. Because the growth of plants is mostly dependent on the features of the soil, digital assessment of various soil variables, classification, and mapping is vital to agricultural approaches such as crop maturity, disease surveillance, and global food production. The classification of soils and mapping of their properties have both made extensive use of remote sensing information. However, because of the low spatial and spectral resolution, there is a need for additional research on multispectral imaging. Because there is not enough bandwidth, multispectral imaging also has a greater degree of spectral uncertainty. In-field hyperspectral data collection and imaging spectroscopy have yielded useful information on the resources of the planet's crust, allowing for the identification of minuscule components of various materials found on its surface. The visible, near infrared, and shortwave infrared ranges (400 to 2500 nm) are covered by the spectra that are provided by hyperspectral data. These spectra are provided in a large number of tiny, continuous spectral bands. In a similar vein, field spectroscopy can serve as an alternative to the traditional laboratory analysis of the characteristics of the soil. Soil scientists in Israel generated maps of soil organic matter, soil moisture, soil salinity, and saturated soil moisture using data from the DAIS-7915 (Ben-Dor et al., 2002) airborne hyperspectral sensor and field spectrometers with 62 soil samples. These maps were based on aerial hyperspectral data. The association between the mineralogical and chemical profiles of the species and the various soil structures was investigated in Brazil using AVIRIS aerial pictures and data from 86 soil samples obtained from Spectral Analysis Device (ASD). Data collected by the Hyperion satellite and the Field Spec Pro spectrometer from several soil samples were used in an analysis of the link between soil salinity characteristics and the impact these parameters have on the spectral features of the soil. A correlation between Hyper-Spec-TIR aerial photography and field data is used to analyze agricultural fields in order to map several soil components (Tarik Mitran et al., 2015). These soil qualities include carbon, silt, aluminum, and iron. The area of land used for this evaluation is 315 acres. In order to evaluate soil erosion utilizing aerial approaches with NOAA/AVHRR data, a correlation was found between the color of the soil and the normalize difference vegetation index (NDVI). The use of linear empirical models allows for the creation of soil maps covering huge areas and the prediction of soil erosion processes. The hyperspectral imaging and Field Spec Pro (ASD) data were utilized in order to identify and categories the clay minerals found in the ground. Clay minerals were detected by XRD analysis, soil spectroscopy, and satellite data (Janaki Rama Suresh, Sreenivas and Sivasamy, 2014) and they were separated from the soil using the XRD method. Random forest regression was employed as the approach to correlate the clay minerals. Monitoring the link between landscape spectra and image data using a regression model was shown to be an effective way to analyze soil qualities and map their distribution. This was discovered through research that was conducted. There are four significant types of soil that have been found on the mainland of India. These are the Indo-Gangetic alluvial soils, the black cotton soils or Regur soils, the red soils that are found on metamorphic rocks, and the lateritic soils. The Indian Soil Fertility Study suggests conducting comprehensive soil research based on the climatic zones of the soil. The importance of the association between different types of soil and crop production in agricultural management cannot be overstated. Studies have been conducted to map soil attributes using hyperspectral data, but the classification of soil types has not been included in these studies. Instead of just mapping soil attributes, one of the goals of this research is to investigate how surface soil classification might be represented across a variety of heterogeneous regions using a library of soil spectra that is derived from physicochemical parameters as well as soil classification (Vibhute and Kale, 2023). Within the scope of this work, unique soil spectral libraries are utilized in order to successively characterize surface soils for the purposes of classification. The spectral library makes use of the distinct physicochemical features of soil, which vary across locations and over the course of time.

2.3 Remote Sensing and Color Analyzation

The color of the soil can be used as a basic index in classification, and this can be done both visually and by remote sensing. For the purpose of carrying out large-scale land mapping, many forms of remote sensing technology, such as multispectral, hyperspectral, thermal infrared, and LiDAR imaging, supply useful data. Scientists are able to precisely map and categorize soils through the use of spectral information as well as changes in thermal properties. Agriculture, land management, environmental monitoring, and the management of natural resources are all areas that benefit significantly from the application of these technologies. In recent years, remote sensing image scene classification, often known as RSISC, has been receiving a growing amount of interest in both academic and practical applications. It intends to organize the photos from the scene into a distinct set of significant land cover and land use classifications based on the information contained within the images. RSISC is an organization that plays a significant part in the world of aviation and the subject of scene classification has been approached using a variety of different approaches, one of which is the analysis of satellite images. For a more in-depth look at the categorization methods and data sets that are conventional for remote sensing scenarios, we can turn to the survey (Cheng, Han and Lu, 2017). The present-day methods for classifying scenes can be grouped into one of three types according to the feature representation that is utilized (Huang et al., 2023b): (1) methods based on manual feature learning, which aim to engineer certain features designed by humans through technical skills or domain expertise; (2) methods based on unsupervised feature learning, which focus on learning a set of basic features for feature encoding, i.e. the input of features is a set of features handcrafted, and the output of features is a set of deeply learned features. Both of these types of methods can be used to learn features for feature encoding. approaches based on learning that automatically learn feature representations of raw data by employing a generic convolutional neural network (Deep CNN) learning procedure. Deep convolutional neural networks (deep CNN) have been put to good use in recent years to solve the challenge of picture classification. This method often produces very high classification accuracy due to the fact that deep CNN is able to extract robust feature representation. powerful for the task of classifying images that are received downstream. Because of this, techniques that are based on deep learning are becoming increasingly common in the field of remote sensing. Some examples of these techniques include change detection of heterogeneous remote sensing images (Wu et al., 2022), hyperspectral image classification (Wu et al., 2020), scene categorization remote sensing images, and so on. Although the majority of earlier deep learning-based methods only used images of remote sensing scenes in the RGB color space to learn how to represent distinguishing features, there are other color spaces, such as Hue Saturation Value (HSV), that can be used here to train some additional CNN models to support the CNN model that was trained with aerial images in the RGB color space. These additional CNN models will support the CNN model that was trained with aerial images in the RGB color space. The representation of discriminative characteristics retrieved by CNN models from images in distinct color spaces has a certain complementarity. (Chen et al., 2021a) In fact, the knowledge of different color spaces is complimentary to one another. As a result, the accurate classification of scenes can be improved further through the strategic combining of information that is complementary across a variety of color schemes.

Over the course of the past few years, a variety of solutions to the RSISC problem have been suggested. They may primarily be broken down into three distinct categories, which are as follows: (1) methods based on the learning of handmade features; (2) methods based on the learning of unsupervised features; and (3) methods based on deep learning. In practice, approaches that are based on manual feature learning concentrate their attention primarily on the design of a variety of human-designed features (for example, spectral information, color, texture, and shape). form or combination thereof) to represent images obtained through remote sensing of environmental conditions. An efficient remote sensing image representation method that is based on a local binary model that is augmented at many scales and fisher vectors was utilized in the development of a method. Another individual suggested a way for obtaining invariant characteristics through the application of global rotation. Several studies have suggested collaborative representation strategies in order to investigate the nature of the complementary relationship between local and global characteristics. However, when compared to unsupervised feature learning-based methods and deep learning feature-based methods, the classification performance of remote sensing image scenes is largely limited by handcrafted features. This is because it is quite difficult for handcrafted features to accurately describe the rich semantic information that is present in remote applications. Please take a picture. This RSISC method type should no longer be used. Many academics have created unsupervised feature learning methods as a solution to the problems that are caused by the limits of handcrafted feature-based methods. Method for classifying scenes acquired via remote sensing. Following the extraction of low-level dense object descriptors, which are then encoded, a method for describing local spatial patterns has been proposed by a few research. conforming to the fundamental functions, a brand-new sparse representation can be created. Bypassing the deep learning phase of satellite image classification is one of the goals of the Two-Layer Sparse Coding (TSC) model's architecture. This goal can be accomplished by discovering the true neighbors of the image. In other research, unsupervised multi-layer feature learning approaches have been presented as a means to automatically generate features spanning from the most basic to the most complex. information about the structural makeup of things, as a response to the hierarchical cognitive function of the human visual cortex. Unsupervised deep feature extraction is an additional method that was recently proposed. This method makes use of a CNN that has been trained with an unsupervised algorithm in order to take advantage of two distinct forms of feature sparsity: population and lifetime rarity. An approach that minimizes the reconstruction error between the input image and the convolution output has been proposed by a number of research. This method makes use of a shallow weighted decoder network to learn a collection of feature maps and filters. Because the majority of approaches that are based on unsupervised feature learning do not incorporate scene class information, also known as supervised information, they are unable to achieve accurate classification at the highest stage in many different scenarios. In recent years, deep learning approaches have garnered attention in the field of remote sensing scene classification (RSISC) as a result of the accessibility of large-scale remote sensing data and the development of high-performance computing resources. This is owing to the fact that deep learning methods are able to more accurately categorize remote sensing images. For instance, Deep Belief Networks (DBNs) have been suggested as a means of selecting effective features that are both more repeatable and discriminative, which ultimately results in high-performance scene categorization (Zou et al., 2015). Another novel approach known as Bag of Convolutional Features generates visual words from deep convolutional features by employing pre-trained CNNs and capitalizing on the power of strong feature representation (Cheng et al., 2017). In addition to this, a metric regularization term has been implemented for CNN in order to map images from the same class to surrounding scenes as well as scenes from different classes. In addition, a framework called the Feature Aggregation Convolutional Neural Network (FACNN) has been developed in order to combine the processes of feature learning, aggregation, and classification training into a unified environment. It is the purpose of the iterative attention framework to reduce high-level spatial and semantic data into more straightforward vectors so that more accurate predictions may be made. It was suggested to use a multi-instance densely connected ConvNet (MIDC-Net), which is capable of achieving state-of-the-art performance while also taking into consideration local semantics (Bi et al., 2020). Researchers have been motivated to develop new methodologies as a result of this strategy. An improved version of the Local Semantic Network, or LSE-Net, has been developed to simulate the human visual perception of important local regions in a remote sensing scene and to construct a more discriminative local semantic representation for improved classification performance (Bi et al., 2021). This has allowed for the effective extraction and utilization of local information. In addition, the All Grains, One Schema (AGOS) framework has been suggested to successfully recognize the region of interest of objects of different sizes and to construct a more discriminative representation for object distributions that are intricate. This has been done with the goal of reducing the amount of computational overhead involved. In reality, deep learning-based approaches frequently obtain more robust discriminative features for subsequent classification tasks than hand-crafted feature-based methods and deep learning-based methods that are based on unsupervised feature learning. This is because deep learning-based methods learn to recognize patterns in data with less guidance from an expert. Therefore, the most often used tactic is the one that involves CNN broadcasting images obtained through remote sensing.

Scene classification is one of the most fundamental applications in the field of remote sensing. The vast majority of datasets used for scene classification typically consist of color photographs, and these images are frequently represented using the RGB color space. Recent years have seen a proliferation of similar methodologies being developed with the purpose of researching the influence of color information in color space on subsequent categorization tasks. They conducted a comparative analysis of the pixel classification performance of two skin detection algorithms over five different color spaces and published their findings. Through the use of deep neural networks, this study studied how the presence of color information affects how well an image can be classified. In addition to this, a number of techniques that make use of various color spaces have also been created. In order to improve the effectiveness of picture segmentation (also known as pixel classification), they devised a novel method utilizing a hybrid color space (HCS), which was defined by the three-color features that were found to be the most discriminating. In addition to this, the adaptive hybrid color space, also known as the AHCS, is built with the use of a sequential supervised feature selection approach. It is used to the problem of soccer picture segmentation and seeks to extract more significant regions from players in order to identify their team with a high level of precision. They performed an analysis on the dependability of the various color spaces, then used the results to address the problem of water partitioning. They investigated the feasibility of identifying plant populations by extracting discriminative features from various color spaces. These methods indicate that changing color spaces can have a major impact on the execution of a future job, and they show that accuracy can be improved by making good use of color information stored in a variety of color spaces. Combining a number of distinct color spaces during the decision-making process might prove to be a more fruitful strategy than the approaches described above. In situations in which the output of the classifier is fuzzy partitions that offer probabilities of membership in multiple classes, it is usual practice to make use of variants of it. Because the results of a soft classification can frequently provide more information than the results of a hard classification, and because kernel aggregation methods frequently work better, several new methods that leverage DS principles have been presented in recent times in order to integrate different classifiers. outperform methods of additive synthesis in their performance. To achieve comprehensive risk assessment in the face of uncertainty, a newly developed method of multi-classification information fusion incorporates a probabilistic support vector machine that makes use of evidence theory. Within the context of a proof-theoretic framework, they proposed a general method for the synthesis of multi-module decisions that might be used to manage large-scale device operating status monitoring. To be more specific, the ultimate state decision is made by combining the results of numerous pieces of soft classification, each of which gives the probability of a distinct operating state across multiple modules, in accordance with the DS rule and the Jensen-Shannon divergence joint efforts. They came up with a radar vision synthesis system that uses evidence theory to merge the soft sensing results given by radar and cameras. This allowed them to classify objects in difficult roadside settings. They suggested a new way of merging the evidence of two sensors for object categorization by employing the DS rule, and the weights of the sensors are adaptively determined by making use of the coefficient of variation. In conclusion, integrating numerous classifiers through the use of evidence theory is not only an appealing technique to integrate multiple sources of information at the level of decision-making, but it also frequently produces higher classification accuracy than some aggregation methods.

A psychophysical phenomenon known as the appearance of color in three dimensions takes place when light strikes an item and is reflected off of it. This causes the object to appear to have color. The term "light" most commonly refers to visible light, which is defined as an electromagnetic wave with a wavelength ranging from around 380 nm to 780 nm and that is able to be recognized by the human eye. In everyday usage, however, the term "light" refers to a different type of light entirely. Some of the light's wavelengths are absorbed when it strikes an object (this is referred to as incident light), while other light wavelengths are reflected off of the object (this is referred to as reflected light). The color of an object can be determined by the wavelength of the light that is reflected off of it. The color of soil, for example, is achieved by reflecting light in the red wavelength band (about 620 to 780 nm), whereas the color of plant leaves is achieved by reflecting electromagnetic waves in the green wavelength band (about 500 to 570 nm).

It has been determined that the hue of the soil is the major characteristic that most accurately reflects both its pedogenic environment and its historical evolution. Both the organic make-up of the soil and the presence of different types of iron oxides are the primary contributors to the color of the soil. The presence of organic matter is responsible for the darkening of the soil, while the presence of iron oxides is responsible for the varying hues seen in the soil. The exact colors are determined by the oxidation state of the iron in the soil. The oxidation state of the iron can be found by testing the soil. Throughout the course of human history, the chromatic qualities of soil have been regarded as an important discriminative attribute among horizons contained within a soil profile and among diverse soil types existing within a certain geographical area. Visually comparing a moist field sample with the chips on a Munsell soil color chart and picking the chip that most closely reflects the color of the field sample is a technique that is often used for doing routine assessments of the color of the soil. This approach may be found in many different types of soil color charts. Due to the fact that it is both quick and does not require any kind of specialist treatment, the measurement of soil color based on appearance can be taken into consideration as a candidate for an appropriate initial screening test for soil discrimination (Schmidt and Ahn 2019). carried out an investigation in which they read and analyzed research publications relating to the hue of marsh soils that were published between the years 1960 and 2018. According to the results of their research, an overwhelming majority of these studies, exactly 81 percent (78 out of 96), used a Munsell color chart as a technique to measure the hue of the soil. This was the conclusion reached by the researchers. The Munsell color system offers a thorough framework for describing color based on its hue, value, and chroma, which are the three basic characteristics that make up color. The term "hue" refers to the most fundamental color, "value" describes the degree of brightness or darkness, and "chroma" denotes the degree to which the most fundamental hue is emphasized. The MSCC is illustrated in figure 1.

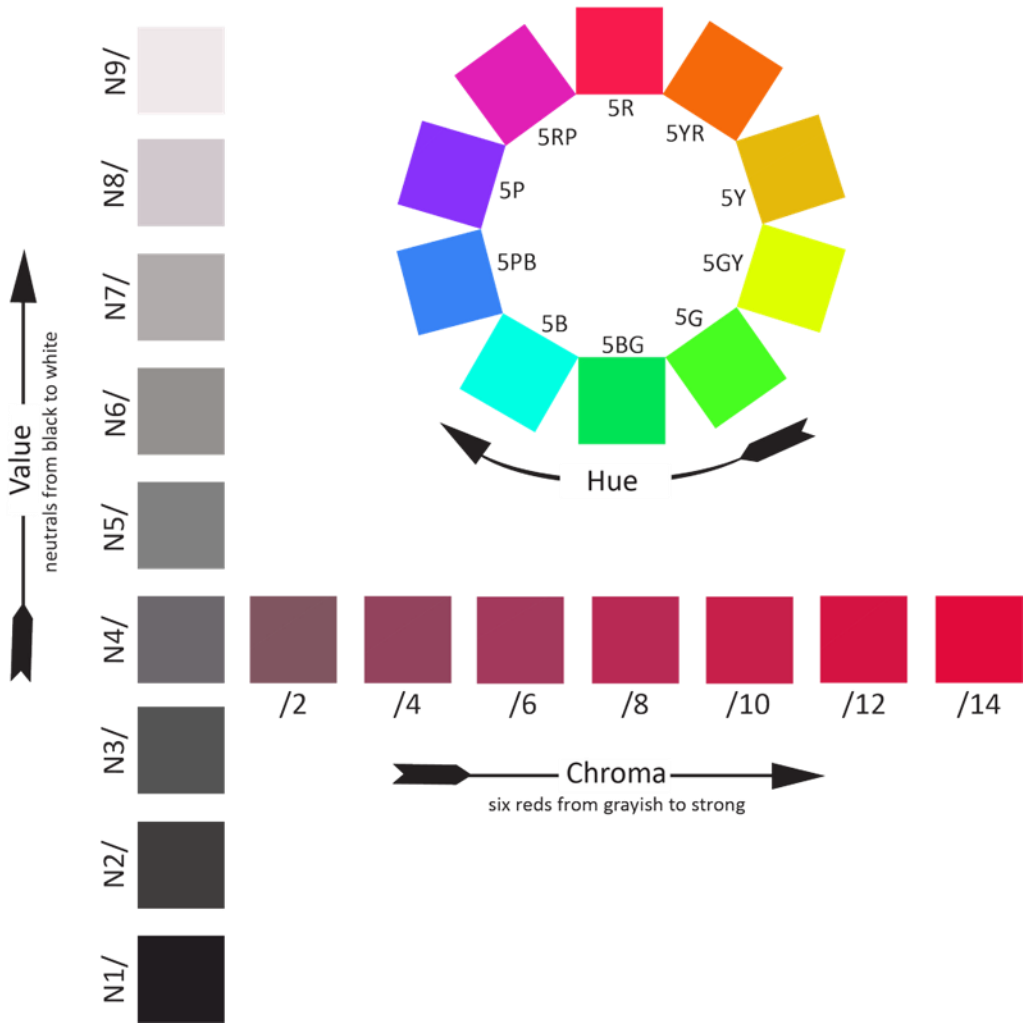

Figure 1: Munsell Color Wheel and Color System. Source: (Schmidt and Ahn 2019).

A color's hue can be categorically described using the letter abbreviation that corresponds to the color's position on the spectrum. The combination YR and Y stands for the color yellow-red, the letter Y stands for the color yellow, and the letter R represents the color red, as an example. The range of values that represent color includes the integers 0 through 10. The hue changes to become more yellow and less red as the number range that each letter range represents grows. This is because the complimentary colors red and yellow provide this effect. A numerical rating can be used to convey the idea of value. This grade has a range from 0 (absolute black) to 10 (absolute white) on a scale from 0 to 10. Chroma can also be expressed in numerical form, where the maximum value of 20 is never reached with dirt and starts at 0 for totally colorless grays (sometimes called the achromatic point). It is common to refer to the achromatic point as the point at which color differences are negligible. There are multiple definitions that can be applied to the term "chroma." In order to classify colors according to equal intervals of visual perception, the Munsell system was created. Since this was one of the main objectives of the system's development, the Munsell system's main advantage is its readability. The Munsell system was created in order to arrange colors according to equal intervals of visual perception, which explains why. Conversely, the Munsell HVC coordinates are psychosensory, meaning that the system is not uniform because they rely on the subjective perception and comparison of the individual. This is one of the causes of the inconsistent Munsell HVC coordinates. The MSCC measurement is essentially arbitrary and subject to a wide range of influences, such as lightness, shadow, soil moisture content, and other related elements. This may also cause the measurement's precision to change. Furthermore, it is critical to remember that MSCC chips show a gradual but noticeable loss of color over time, resulting in undesirable changes to hue, value, and chroma. It experiences this during the course of its lifetime. (Sanchez-Mara n'on et al. 2005) claim that these changes cause inaccurate and inconsistent measurements of the soil's hue. Based on the information presented in (Mouazen et al. (2007)), one could conclude that visual perception is not a dependable method for reliably evaluating soil color. The offered findings allow for the reaching of this conclusion. Because of this, scientists and researchers that focus on soil science have thoroughly examined a broad range of techniques in an effort to identify and quantify soil color as well as predict soil characteristics that are strongly linked to changes in soil color. This is primarily because a variety of soil properties, such as nutrient content and water retention, can be inferred from soil color.

An additional method that may be applied in order to analyze the different hues of soil is the use of the RGB color space. This is among the alternatives that you can choose from. The RGB color model is composed of the primary colors red (R), green (G), and blue (B). Yellow (Y) is the third primary color. By adding to or subtracting from the spectrum of the three main hues—red, green, and blue—one may produce any color, according to this idea. Certain wavelengths allow for the observation of the monochromatic primary stimuli, specifically at 700 nm, 546 nm, and 436 nm, respectively. The numerical values that are allocated to each component of the tristimulus—that is, R, G, and B—in a digital system with eight bits of memory, in order to characterize the color, range from 0 (which represents darkness) to 255 (which represents whiteness). Put otherwise, 0 denotes total darkness, whereas 255 denotes total whiteness. In other words, 0 represents total darkness, and 255 represents whole lightness. In other words, total brightness is represented by 255 and absolute blackness by 0. Drawing from the results of several studies, it has been determined that the three fundamental colors—red, green, and blue—when combined produce a spectrum with a total of $(2^8)^3$ distinct color tones (R.A. Viscarra Rossel 2006). The color spectrum of the system can be graphically depicted as a three-dimensional cube with orthogonal dimensions that align with both the RGB color model and the Cartesian coordinate system. You can think of this cube as a color space. This cube is observable from any side from any other side. Next, depending on the option selected, a point of the relevant color is assigned to be displayed somewhere on the cube's surface or inside its bounds, as seen in figure 2 below. This could be anyplace on the cube's exterior or inside its boundaries.

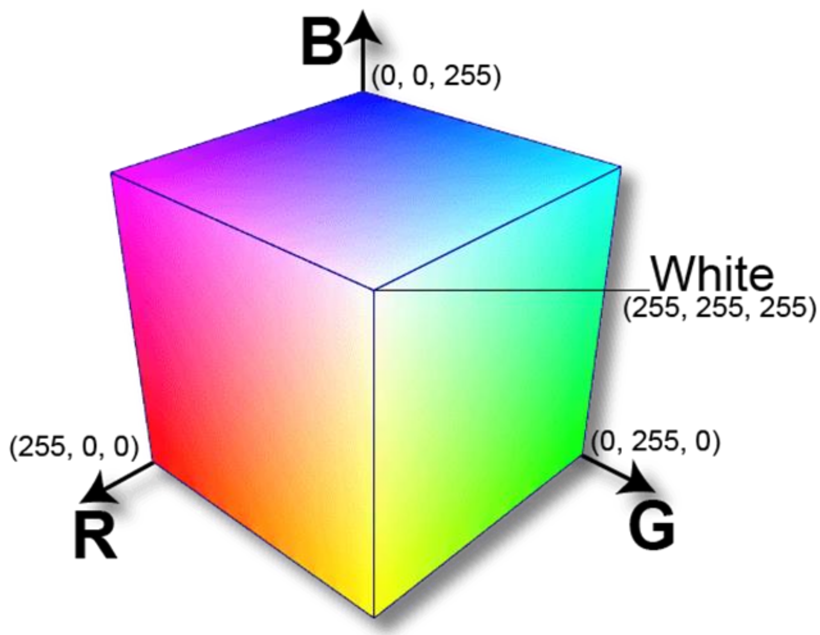

Figure 2: RGB Color Model. Source: (R.A. Viscarra Rossel 2006).

The major diagonal encompasses all of the imaginable shades of gray, ranging from black (R = G = B = 0) to white (R = G = B = 255), as well as from the absence of color to the presence of the color with the highest possible intensity.

Unfortunately, the lack of established color references has made it difficult to use soil color as a means of expressing soil properties (Kirillova et al., 2018). This has been a barrier to the use of soil color in this capacity. The use of soil color as a technique of distinguishing between different soil properties has grown increasingly difficult. As a consequence of the continuous development of colorimetric methodology throughout the course of time, the International Commission of

Illumination (CIE) decided it was necessary to establish soil color standards (Morgan et al. 2009). In 1931, the Commission Internationale de l'Eclairage (CIE) began its effort to standardize the numerous color order schemes that were in use at the time. These schemes were in use at the time because the CIE wanted to standardize them. In order to accomplish this, it was necessary to provide the light source, the observer, and the method that was used to determine the values that are used for expressing color. It was during this time in history that the XYZ color system became extensively used, and its use has not ceased since that point in time in the annals of human history. In this specific system, the brightness or luminance of the color is expressed by the variable Y, which is used to represent the value. This particular variable also serves to represent the value. On the other hand, the variables X and Z are employed to represent virtual components of the primary spectra. Virtual components of the primary spectra are components of the spectrum that are conceivably attainable in theory but cannot be realized in the actual world. The illustration can be found below in figure 3.

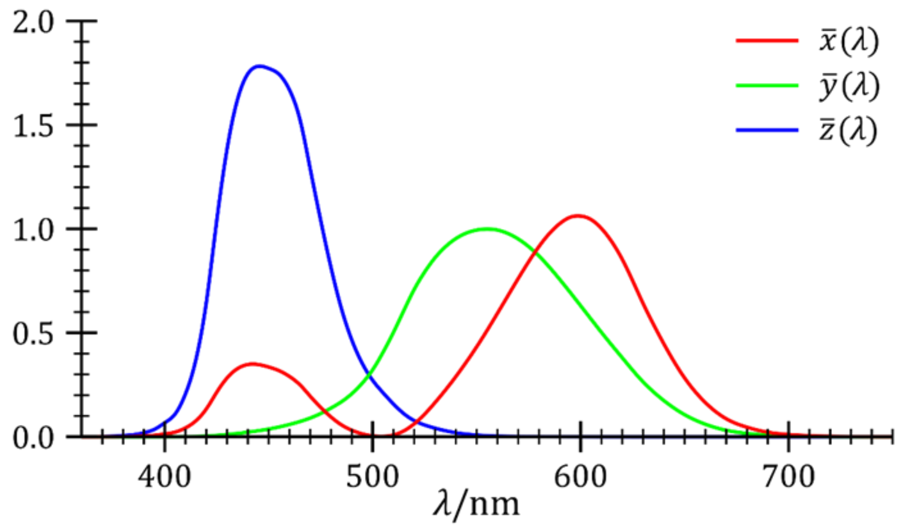

Figure 3: CIE XYZ Color Space; Source: (Morgan et al. 2009).

It is notable that the application of XYZ tristimulus values in the field of color definition is useful; nevertheless, it can be difficult to identify the impact these values have on perception. The International Commission on Illumination (CIE) established the Yxy color space in 1931 as a way to represent color in a manner that was only two-dimensional (R.A. Viscarra Rossel 2006). This study was carried out in an effort to find a solution to the problem that was brought to light. Changes in brightness, Y, do not affect the chromaticity coordinates, x and y, which denote color variations extending from blue to red and from blue to green, respectively. The xy chromaticity diagram that has been supplied below can be understood to be a visual depiction of the color that is present in the image. This representation of color can also be viewed visually as shown in figure 4.

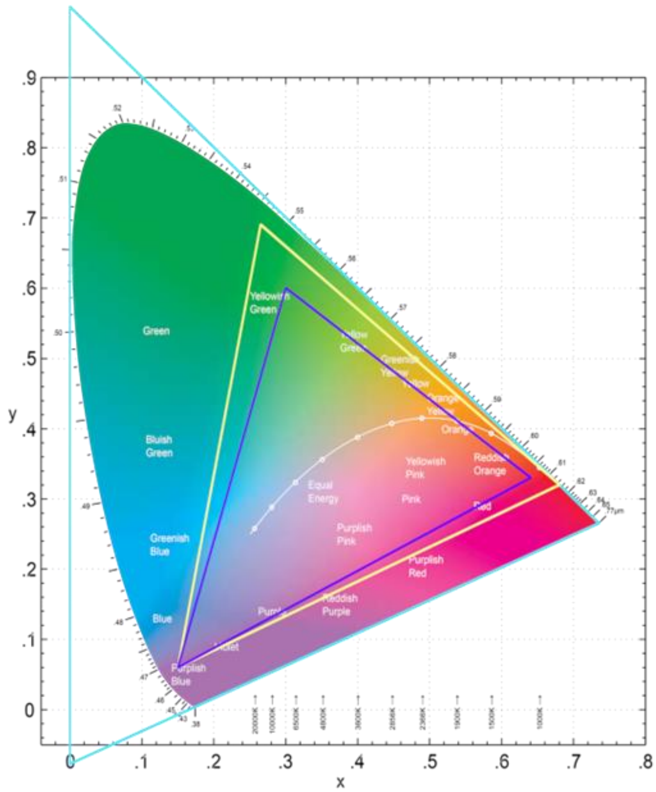

Figure 4: CIE Yxy Chromaticity Diagram; Source: (R.A. Viscarra Rossel 2006)

The discrepancies that can be seen between the color distinctions that are seen and the actual arrangement of colors inside the framework is a key limitation of the CIE chromaticity diagram. This limitation is one of the primary reasons why the CIE chromaticity diagram is so complex. The fact that there is a hole in the diagram is one of its shortcomings. Both the Yxy and XYZ coordinate systems allow for the observation of the phenomenon known as perceptual non-linearity.

In 1964, the International Commission on Illumination (CIE) developed the CIELUV system in order to address the perceived non-linearity of the XYZ and Yxy systems. This was done in order to solve the perceived non-linearity of these systems. In order to shed light on the problem at hand, a study like this one was carried out. According to (Wyszecki and Stiles 1982), the construction of the CIELUV system is the consequence of transforming xy coordinates into a standardized chromaticity scale. This transformation takes place when xy coordinates are transformed. The formation of the conceptual structure was supposed to be the result of this endeavor. The CIELAB color system was designed with the purpose of achieving the highest possible level of consistency in the representation of colors. In order to determine the values, nonlinear changes are applied to the XYZ coordinate system. The metric lightness function, which is denoted by the symbol L and indicates brightness or luminance, is the same in each of these different grading systems. The function in question is utilized frequently in both of these systems, and it displays a numerical scale with a range that goes from 0 (representing black) to 100 (representing white). The red-green scales and the blue-yellow scales of an opponent are represented by the chromaticity coordinates a*, b*, u*, and v*, respectively. The red-green scales are represented as (+a, +u for reds and a, u for greens), while the blue-yellow scales are represented as (+b, +v for yellows and b, v for blues).

In the present day, one of the most common methods that is used is one that involves making color determinations on bulk soil samples after they have been air-dried. Despite this, there have been calls for the development of methods that are significantly more complex in order to determine color. The color of a bulk soil sample can primarily be ascribed to the presence of clay particles, which are tightly connected with soil humus to form the clay-humus complex, as well as clay particles coated with iron oxides. Additionally, the existence of clay particles can also be attributed to the presence of iron oxides. As a consequence of this, a number of forensic soil analysts believe that color evaluations have to be concentrated on the clay component of the soil. The production of the clay-humus complex, which may be attributed to the intimate binding of clay particles with soil humus, is what can be said to be responsible for the presence of the clay fraction. Previous research carried out by forensic soil analysts have suggested a methodology in which the color of a soil sample is evaluated after a series of preparatory steps, including air-drying, removal of moisture, elimination of organic matter, extraction of iron oxide, and finally, ashing (R Zeng). This methodology was proposed as a result of studies that were carried out in the past. The geographical provenance of the soils being investigated is an important factor in determining whether or not these treatments are effective in promoting color difference between soils that originate from various places.

In addition to methods that rely on the human eye, numerous studies have proved the substantial capabilities of digital cameras, particularly those that are integrated into mobile phones, for the aim of swiftly analyzing the color of the soil. This is done for the same reason as the use of procedures that rely on the human eye. However, the hue of a picture of dirt captured by a digital camera is vulnerable to change based on the lighting conditions that are already present in the surrounding region. This is because digital cameras capture light differently than film cameras. According to (Kirchner, Koeckhoven, and Sivakumar 2018), in order to increase the accuracy of color measurements, it is essential to make use of additional methods, such as making use of a reference gray card for color correction. This is one example of a strategy that can help improve the accuracy of color measurements. In a laboratory context, one may use a spectrophotometer or colorimeter in order to acquire an assessment of the color of the soil that is both more accurate and more objective. This can be performed by making certain that suitable white standards are used, as well as by methodically preparing soil samples. (Kirchner, Koeckhoven, and Sivakumar 2019) discovered that throughout the course of the previous decade, a number of one-of-a-kind colorimeters have been developed and made available on the market at prices that are lower than the threshold of 500 US Dollars. These colorimeters may be obtained in a variety of price ranges. A large portion of these colorimeters are constructed with a tristimulus color sensor and an LED light source as the fundamental elements of their construction, respectively. They were conceived from the ground up to be operated wirelessly by way of a Bluetooth connection established between a mobile device, such as a smartphone or tablet, and the controller app installed on the device. You may get your hands on some of these items at prices that are lower than one hundred US dollars per. Because of the exponential increase in the number of people using smartphones around the world, it is now possible for a diverse range of users, including individuals who are not part of the scientific community, to measure the color of an object at a price that is within their financial reach. This progression has also been helped along by the accessibility of colorimeters that are reasonably priced. The utilization of these technologies made it possible for anyone who did not possess the necessary level of specialized expertise, such as farmers, gardeners, and students, to quantitatively evaluate the color of the soil. This was a significant advancement in the field. They were able to acquire knowledge regarding the relationship between the color of the soil and the contents of the soil as a result of this, and they were subsequently able to use the data that they obtained in order to categorize the soil.

3. METHODOLOGY

This section provides an extensive description of the experimental methodology, outlining the sequential steps involved in selecting the research location, collecting soil samples, documenting soil color at various stages, and analyzing the collected data. In addition, it discusses the equipment and techniques employed throughout each stage of the experiment.

3.1 Color Analyzing

The utilization of numerical values to depict the color of an item is facilitated using a notation system known as a color space model. This particular model is alternatively referred to as the A color model. The choice of using either a three-dimensional space or a one-dimensional axis as the foundational structure for the color space is contingent upon the specific model being employed. Several color space models often used in many fields include CIE XYZ, CIELAB, and RGB. There is a substantial increase in quantity. In the context of color space models, a specific color can be represented by a point located either on a one-dimensional axis or within a three-dimensional space. Both of these representations are considered to be reasonable. The RGB color scheme is extensively employed in electronic devices, such as digital cameras. The reason for this is that the RGB color model provides the most precise and faithful representation of colors. The reason for this is that the RGB color space yields the most accurate depiction of reality. This technique of color communication utilizes the three primary colors of light, denoted by the letters "R," "G," and "B." The colors red, green, and blue are also denoted by these respective letters. The three letters, namely "R," "G," and "B," are commonly denoted as the RGB color model. In an alternative formulation, it can be asserted that any chromatic shade can be delineated by means of the color that ensues from the amalgamation of the primary hues of red, green, and blue. The act of enhancing the brightness of a color by incorporating extra red, green, or blue is referred to as "additive mixing." This terminology is also employed to describe the action of doing this procedure. The phenomenon is alternatively known as "additive mixing". The efficacy of the RGB color space model in faithfully and efficiently reproducing a vast percentage of colors is the primary factor contributing to its formidable capabilities. The strength of the model derives from its capacity. However, it should be noted that the RGB color space model does not possess the capability to comprehensively encompass the entire spectrum of hues that may be detected by the human visual system. The rationale for this is because RGB is an acronym that represents the primary colors red, green, and blue. Another issue arises from the fact that the RGB values yield a wavelength that deviates from the wavelengths seen by cone cells responsible for human vision. The phenomenon of color perception in humans is mostly attributable to the presence and functionality of cone cells. Differentiating between the different wavelengths can be a significant challenge. The presence of this phenomenon results in the establishment of an obstacle. Cone cells are capable of detecting light across the entire spectrum of wavelengths, encompassing short (S), medium (M), and long (L) wavelengths. Consequently, in 1931, the Commission Internationale de l'Eclairage (CIE) developed the CIEXYZ color space model (Morgan et al. 2009). The aforementioned model possesses the capability to represent a wide range of colors discernible by individuals, as it relies on tristimulus values that correspond to cone cells present in the human retina. The utilization of the CIEXYZ color space model in engineering calculations presents challenges due to the presence of perceptual non-linearity in quantifying the perceptual distance between colors as experienced by humans. This issue has been extensively investigated through numerical and statistical studies of colors. This is the case since the process of color analysis in engineering computations encompasses the utilization of both numerical and statistical analysis techniques. The utilization of the CIEXYZ color space model in engineering simulations poses significant challenges. The genesis of this specific color space model may be traced back to the CIEXYZ color space model. The CIELAB color space model has a high degree of homogeneity from a perceptual standpoint, which distinguishes it from the CIEXYZ color space model. Both of these principles are utilized in order to establish discrete color spaces. In the CIELAB color space model, colors are represented by the combination of three variables: L*, a*, and b*. The development of this model is under the purview of CIELAB. The luminosity of a color is represented by its L* value, which spans from 0 (representing a very dark shade) to 100 (indicating an exceptionally brilliant hue). A number of 0 signifies the darkest color, while a value of 100 represents the brightest shade (Morgan et al. 2009). The color is represented by the variables a* and b*, where a* represents colors that are closer to red (positive) or green (negative), and b* represents colors that are closer to yellow (positive) or blue (negative). Scalar numbers are denoted by the variables a* and b*. The values denoted as a* and b* are commonly associated with color representation. As depicted in figure 5, the three-dimensional CIELAB color space visually represents each color as a point within its framework.

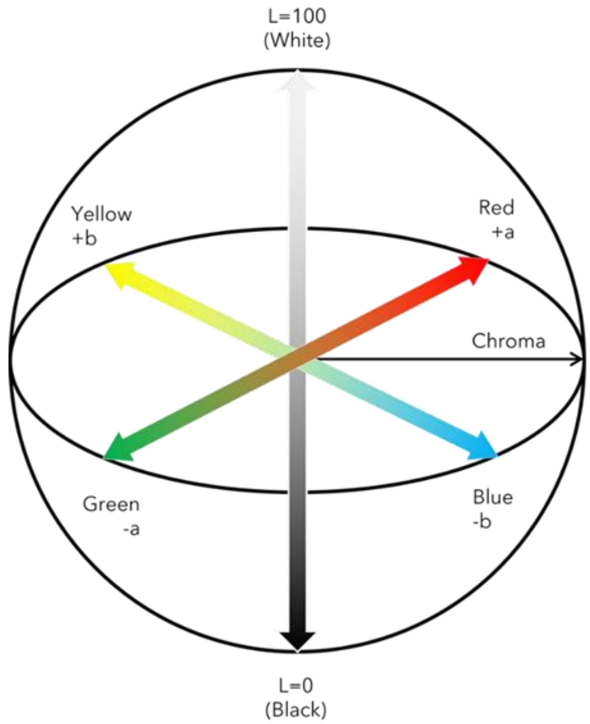

Figure 5: Three-dimensional CIELAB color; Source: (Morgan et al. 2009)

The CIELAB color space model has not been widely utilized in soil image analysis, in contrast to the RGB color space model. However, the CIELAB color space model offers the capability to represent colors by separating color components into "lightness" along the L*-axis and "chromaticity" on the a*-b* plane. The utilization of the CIELAB color space model enhances the precision in representing color. Consequently, it is expected that this technology will prove valuable in addressing discrepancies in soil color resulting from alterations in lighting conditions. Illuminance, which denotes the level of light brightness, and color temperature, which signifies the chromaticity of light, are the factors contributing to these variances.

The primary objective of the current investigation was to evaluate the soil properties utilizing the CIELAB methodology. The saturation levels of the color were evaluated across a spectrum, spanning from maximum saturation to minimum saturation, with the aim of utilizing this approach to anticipate the properties of the soil. The research employed varied values of L, a, and b at specific saturation stages to evaluate the changes in soil properties across varying amounts of moisture.

The researchers (Aitkenhead et al. 2017) have developed a cost-effective spectrophotometer with the ability to operate inside the visible spectrum. The experimental setup consists of several components, including a tungsten light source, multiple mirrors, a diffraction grating, and a digital camera. These elements are utilized to capture the visible spectrum of soil samples. Henceforth, the color sensor denoted as the Nix Pro^{TM} shall be henceforth referred to as the Nix Pro. The Nix Pro device was developed by Nix Sensor Ltd., a company based in Ontario, Canada. As depicted in figure 6, the device under consideration is a colorimeter that can be classified as cost-effective.

Figure 6: Nix Pro^{TM}; Source: (Aitkenhead et al. 2017)

A study conducted by (Stiglitz et al. 2016b) employed the Nix Pro device to evaluate soil color shortly after its release to the general public in 2015. The study findings revealed a significant positive relationship between the cyan-magenta-yellow-black (CMYK) color codes derived from 31 soil samples. These samples were sieved to a size of 2 mm and measured under dry and moist conditions using the Nix Pro device. Moreover, the CMYK color codes obtained from the Nix Pro exhibited a strong correlation with the color codes obtained from a conventional colorimeter (CR-400, Konica Minolta, Tokyo, Japan) and those determined through a visual method employing a Munsell soil color chart. Based on the findings of this study, the utilization of Nix Pro for the purpose of soil color analysis appears to present a viable and feasible alternative to established conventional methodologies. Upon conducting a more extensive analysis of the data, it was ascertained that the K% (blackness) values obtained from the Nix Pro device exhibited a notable decrease in comparison to the K% values acquired from the CR-400 device. The K% values exhibited comparability among themselves. Due to this circumstance, a direct comparison between the soil color data acquired from the Nix Pro device and the data obtained from the CR-400 equipment was rendered unfeasible.

The Nix Pro device was employed for the purpose of quantifying color at various levels of saturation. A total of five measurements were performed at each stage in order to enhance the reliability of the findings. The Nix color sensor, developed in Hamilton, Ontario, Canada, has been widely embraced in the field of soil research in recent years. The efficacy of this sensor as a tool for the quantitative, timely, and cost-efficient prediction of diverse soil characteristics has been demonstrated. The utilization of this technology can be done either independently or in combination with other proximate soil sensors. The duration of the scanning process is less than 2.5 seconds, which enables efficient collection of soil color data. The data collected is kept in various color space models, thereby improving its usability and interpretive capabilities. The object's concave base, which is enclosed, has been specifically intended to promote consistent performance in many environments, including both indoor and outdoor settings. This design feature serves to exclude any unwanted interferences and stray light that may affect the object's performance. This particular functionality facilitates optimal performance of the system in diverse environments. The assemblage of components with a dark hue possesses the capacity to augment specific attributes of the soil.

3.2 Territory

Soil samples were gathered from a cereal field at the Hungarian University of Agriculture and Life Sciences (MATE), Gödöllő, throughout the post-harvest period spanning from August 2023 to October 2023. The samples were obtained without any disturbance. As seen in the following figure, the location of the field site was just next to the MATE Gödöllői Kollégiumok Igazgatóság. The precise coordinates of this location are as follows: latitude 47.59705229477654 and longitude 19.366226242690015.

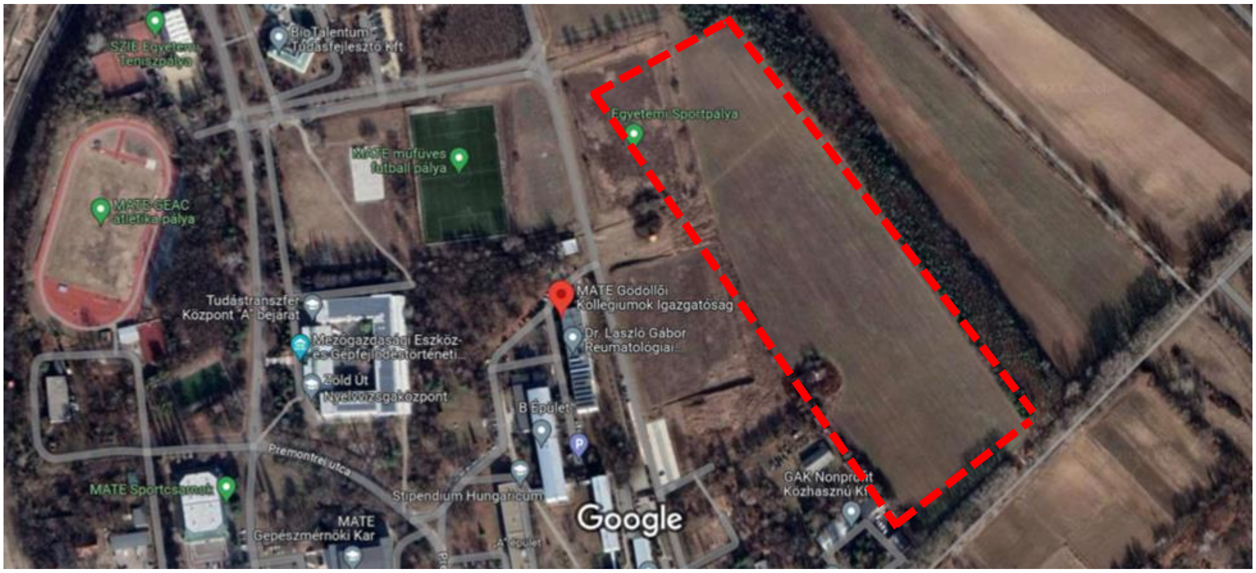

Figure 7: Cereal field, Hungarian University of Agriculture and Life Sciences (MATE); Source: googlemap.com

3.3 Soil Sampling

The techniques that were utilized for analyzing and drying of soil samples included the utilization of aluminum cans that had open ends, and the height of each can was six centimeters. The containers were filled with soil samples that were going to be examined and they were being placed into the containers. After that, the next step in the experimental protocol involved carefully placing three cans each time onto an oven tray, which was then inserted into an electric oven that had been preheated to a temperature of 250 degrees Celsius. After that, the cans were allowed to be heated for the specified amount of time. Because they were left in an environment with a high temperature for a period of time equaling two hours, the soil samples were completely dried out. The oven tray that contained the cans was carefully removed from the microwave at regular intervals of half an hour's duration with utmost caution. The whole experimental procedures and steps carried out in this study were very thorough in its observational work and meticulous in its documentation of the changes in soil color that occurred within the containers at each of the several time periods that were indicated. The progress of the drying process was evaluated by regularly observing the color of the soil. This provided the ability to determine when the soil had reached the desired amount of dryness when the drying process was complete.

The Nix color sensor was utilized in order to get an accurate reading of the color of the soil. The Nix sensor is outfitted with two LED sources that are angled at a 45-degree angle with respect to the sample in order to ensure that the lighting conditions are optimal. An application on the user's mobile device was used to control the sensor. The process of scanning was carried out by leveraging Bluetooth technology and the Android program "Nix Toolkit." This application was installed on an Android handset, specifically the OnePlus Nord 10 model. The scanning was carried out successfully. As was said earlier, the soil samples were evenly spread across the surface of an aluminum container. The color indices that were retrieved from Nix were obtained using a method that involved sliding the sensor over the soil sample five times, once each time the sample was withdrawn from the oven. This allowed the color indices to be extracted. Before each successive sample collection, the appropriate precautions were put into place to remove dust from the Nix instrument in order to avoid the accidental mixing of soil samples or any potential contamination. This was done in order to prevent any potential issues. After that, the subsequent analyzes utilized the five data points that were gathered at each stage for each individual container, and the average of those five data points was utilized. Nix is distinguishable from other color models by its capacity to create results in a wide variety of color models, including RGB, CIEL*a*b*, XYZ, and CMYK, as well as its spectral range of 380–730 nm, its illuminant D50, its 2-standard observer, and others. As part of the experiment, repeated scans needed to be run in order to assess the level of precision or repeatability offered by the Nix sensor. This was accomplished by selecting five sets of soil samples at random, then utilizing the Nix sensor to conduct five successive experiments on each of the selected soil samples.

3. STATISTICAL ANALYSIS

The experiment was conducted on five times, during which soil samples were gathered in three distinct sets and subsequently transferred into three aluminum cans. After each iteration of the experiment, in accordance with the methodology described in previous section, the data was taken from the Nix library and stored as an excel file.

Initially, the data analysis solely focused on the values of L, a, and b. During each experimental trial, the material was subjected to a total of five scans at every saturation stage. The mean value for each step was computed in Microsoft Excel using the formula =AVERAGE(A1:A5) upon completion of each stage. The values of “L”, “a”, and “b” were plotted on a scatter graph, and a logarithmic trend line was fitted to the data. This procedure was conducted for every individual can throughout each respective saturation stage.

The L values at each saturation stage of the three cans for each experiment were plotted on a single graph using a Microsoft Excel worksheet. This was done in order to evaluate whether or not there was a correlation between the values across all cans. The values of the variables a and b were analyzed using methods that were very similar to one another. After the L, a, and b values had been examined, the average of the RGB values was then analyzed using the same methods within the Microsoft Excel worksheet. This was done in order to determine whether or not there had been any significant change that can play important role in this study.

4. RESULTS

This chapter will present the findings of the experiment through the use of graphical representations. During each stage of the experiment, the Nix Pro device was used to measure soil color for each can five times. The table presented below records only the averages of the data obtained from five readings at each stage for each can with stage V representing the lowest moist state and stage I representing the highest moist state.

Soil Samples		L	a	b
Can 1	Stage V	28.32	4.88	11.74
	Stage IV	20.26	5.03	9.02
	Stage III	14.72	1.25	7.62
	Stage II	12.96	2.00	7.07
	Stage I	15.96	4.93	8.04
Can 2	Stage V	26.52	5.39	10.80
	Stage IV	16.68	6.04	7.82
	Stage III	15.74	1.18	7.13
	Stage II	13.72	1.53	6.04
	Stage I	13.72	3.18	7.39
Can 3	Stage V	25.34	4.46	9.31
	Stage IV	15.00	0.84	6.76
	Stage III	14.13	2.26	6.15
	Stage II	11.71	2.63	6.87
	Stage I	10.56	3.65	7.67

Table 1: Average of "L", "a", and "b" Values of Experiment 1.

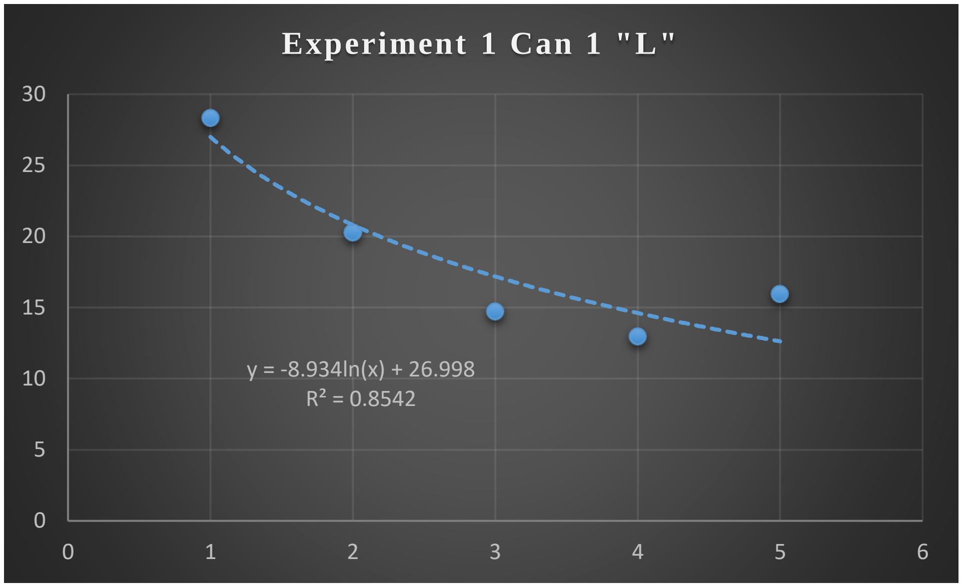

Figure 8: Average of "L" values of Can 1 Experiment 1.

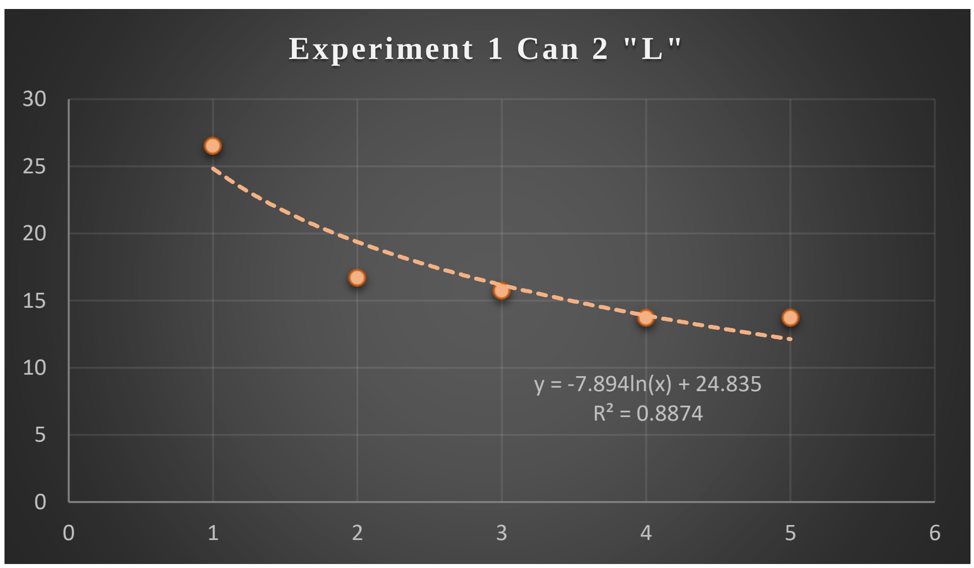

Figure 9: Average of "L" values of Can 2 Experiment 1.

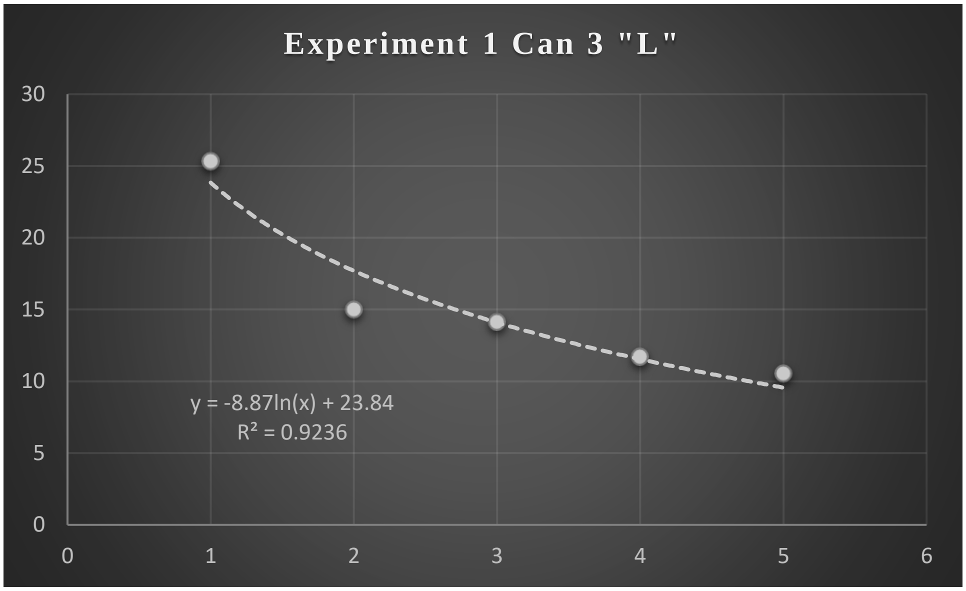

Figure 10: Average of "L" values of Can 3 Experiment 1.

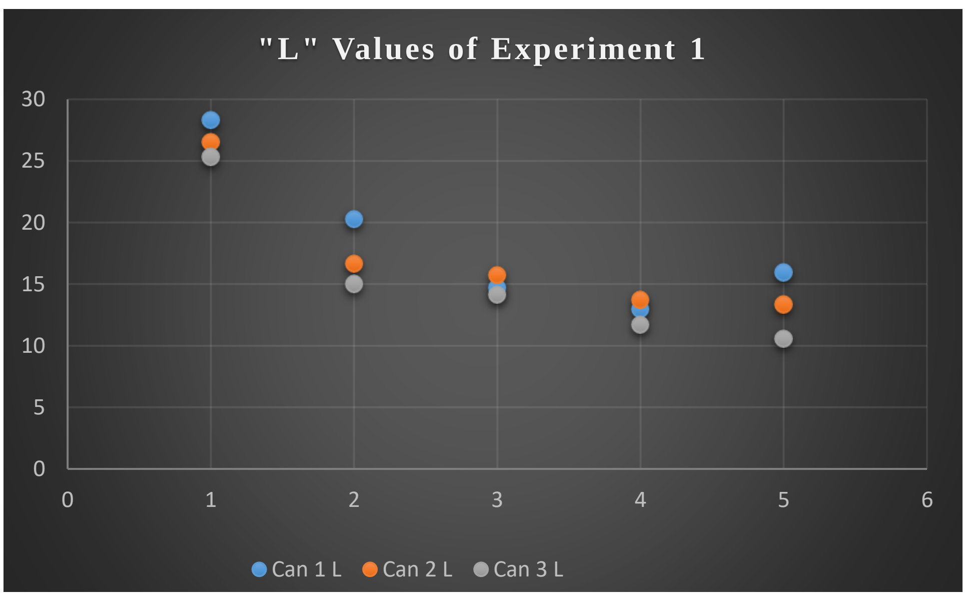

Figure 11: Average of "L" values of Experiment 1.

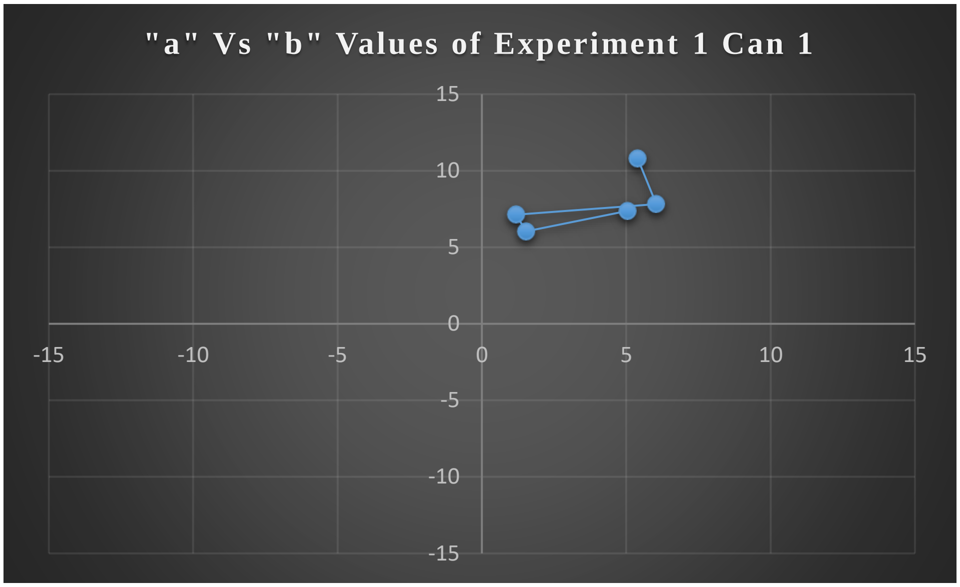

Figure 12: "a" Vs "b" Values of Can 1 Experiment 1.

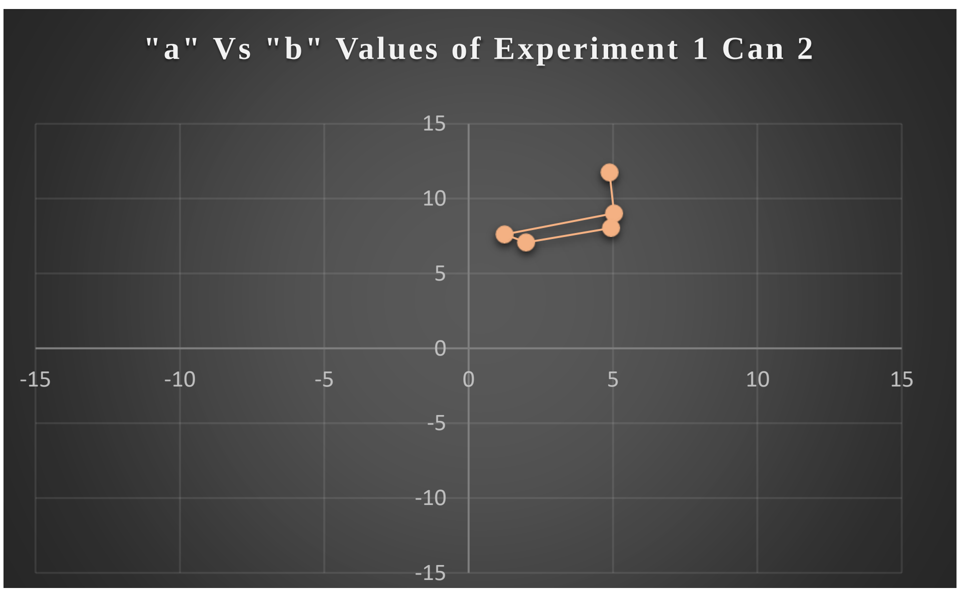

Figure 13: "a" Vs "b" Values of Can 2 Experiment 1.

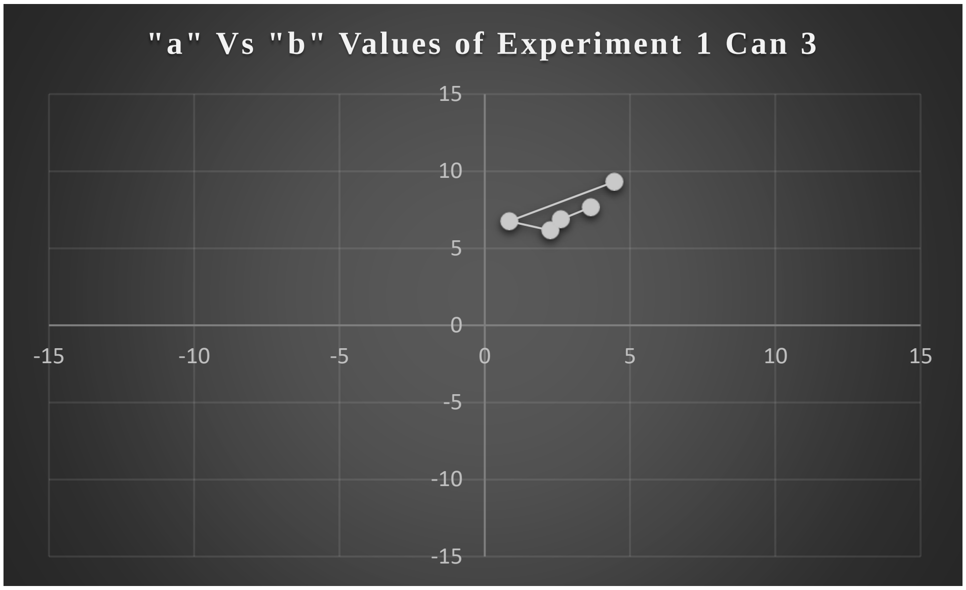

Figure 14: "a" Vs "b" Values of Can 3 Experiment 1.

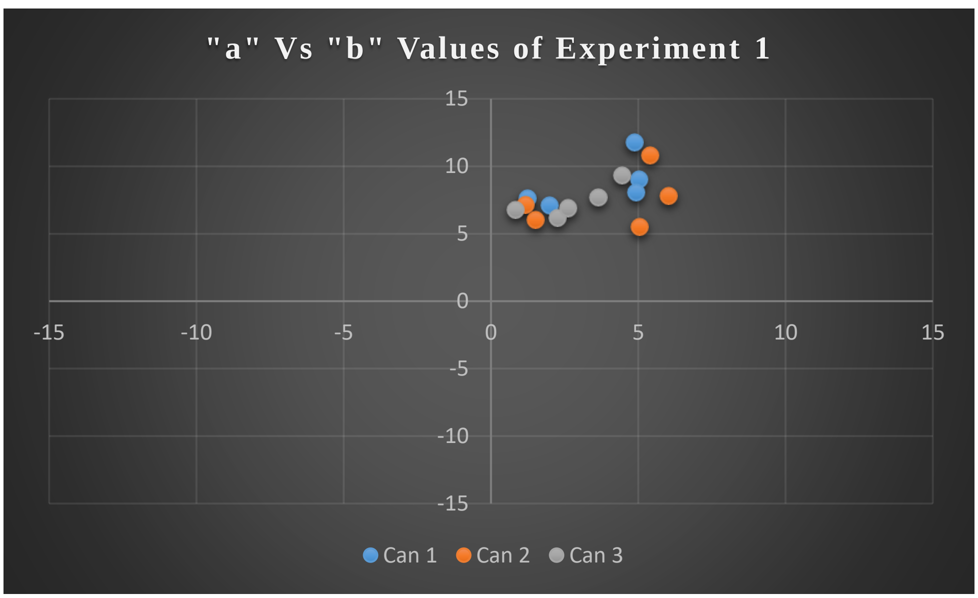

Figure 15: "a" Vs "b" Values of Experiment 1.

The experiment has been conducted an additional four times. The tables and graphs with the average values are presented below.

Soil Samples		L	a	b
Can 1	Stage V	31.152	5.368	12.914
	Stage IV	22.286	5.533	9.922
	Stage III	16.192	1.375	8.382
	Stage II	14.256	2.204	7.777
	Stage I	17.556	5.423	8.844
Can 2	Stage V	29.172	5.929	11.88
	Stage IV	18.348	6.644	8.602
	Stage III	17.314	1.298	7.843
	Stage II	15.092	1.683	6.644
	Stage I	15.092	3.498	8.129
Can 3	Stage V	27.874	4.906	10.241
	Stage IV	16.512	0.924	7.436
	Stage III	15.543	2.486	6.765
	Stage II	12.881	2.893	7.557
	Stage I	11.616	4.015	8.437

Table 2: Average of "L", "a", and "b" Values of Experiment 2.

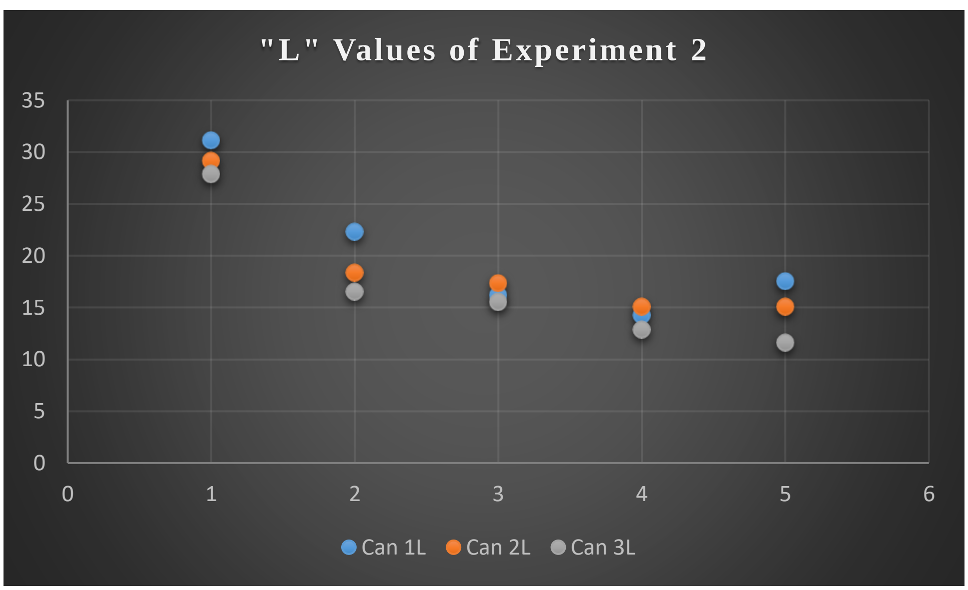

Figure 16: Average of "L" Values of Experiment 2.

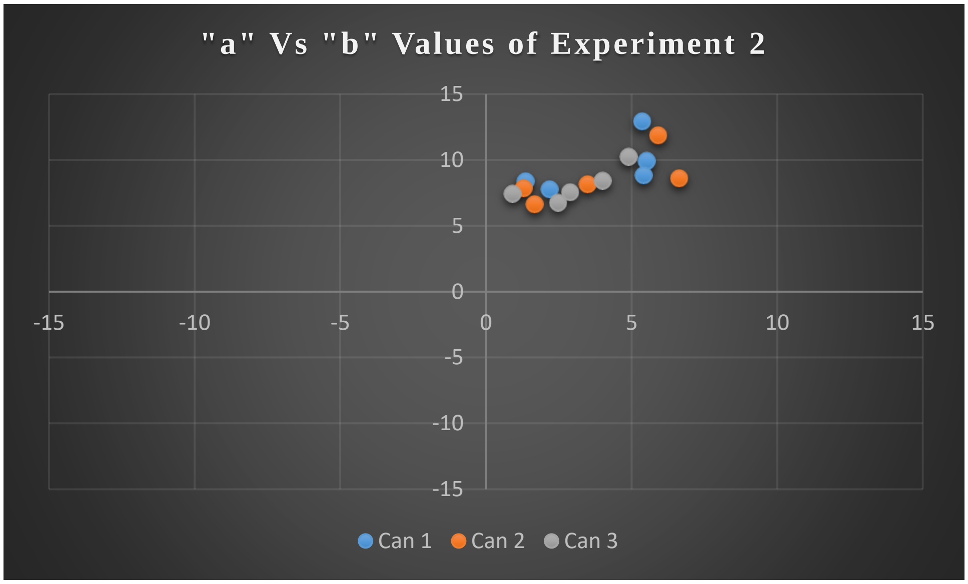

Figure 17: "a" Vs "b" Values of Experiment 2.

Soil Samples		L	a	b
Can 1	Stage V	27.4704	4.7336	11.3878
	Stage IV	19.6522	4.8791	8.7494
	Stage III	14.2784	1.2125	7.3914
	Stage II	12.5712	1.914	6.8579
	Stage I	15.4812	4.7821	7.7988
Can 2	Stage V	25.7244	5.2283	10.476
	Stage IV	16.1796	5.8588	7.5854
	Stage III	15.2678	1.1446	6.9161
	Stage II	13.3084	1.4841	5.8588
	Stage I	13.3084	3.0846	7.1683
Can 3	Stage V	24.5798	4.3262	9.0307
	Stage IV	14.585	0.8148	6.5572
	Stage III	13.7061	2.1922	5.9655
	Stage II	11.3587	2.5511	6.6639
	Stage I	10.2432	3.5405	7.4399

Table 3: Average of "L", "a", and "b" Values of Experiment 3.

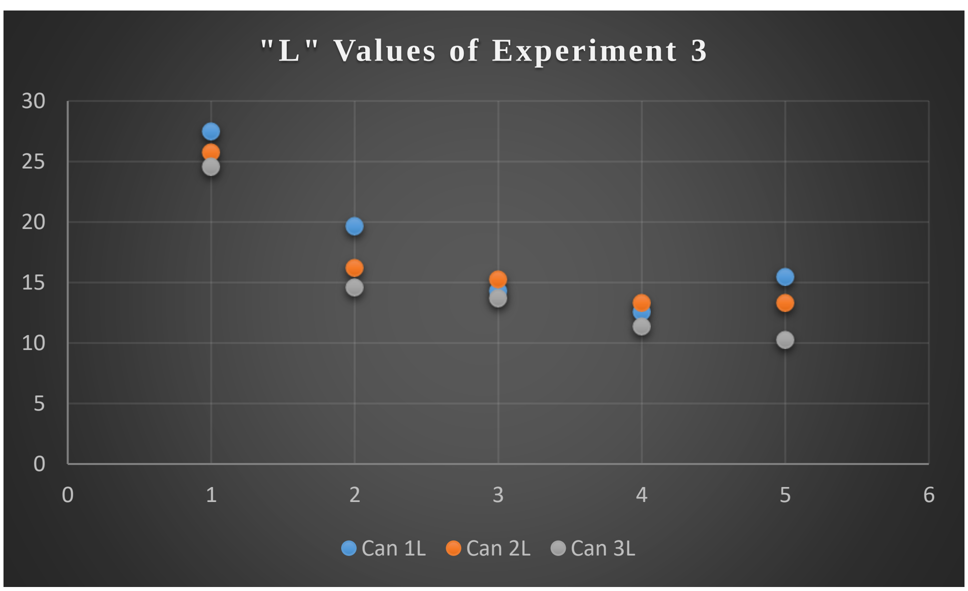

Figure 18: Average of "L" Values of Experiment 3.

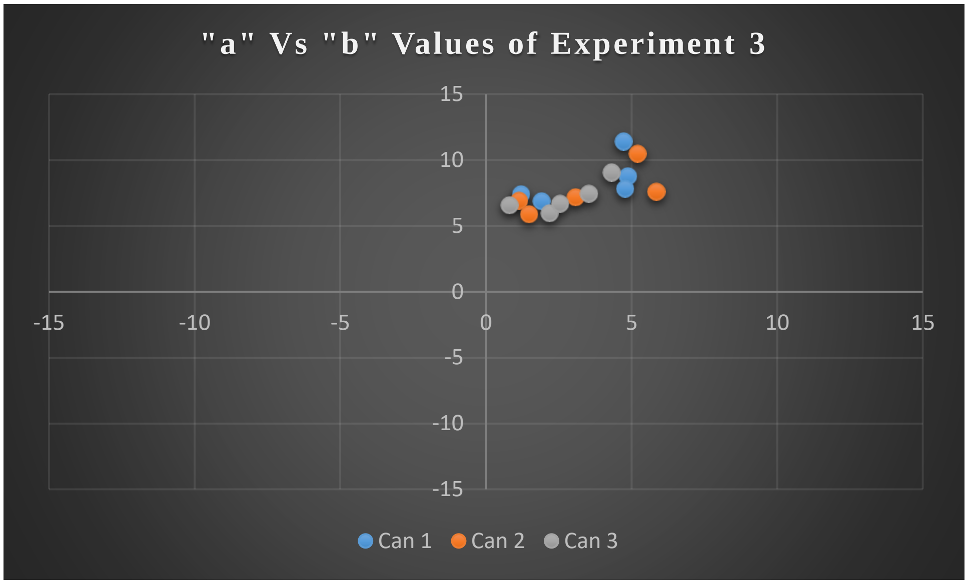

Figure 19: "a" Vs "b" Values of Experiment 3.

Soil Samples		L	a	b
Can 1	Stage V	30.5856	5.2704	12.6792
	Stage IV	21.8808	5.4324	9.7416
	Stage III	15.8976	1.835	8.2296
	Stage II	13.9968	2.516	7.6356
	Stage I	17.2368	5.3244	8.6832
Can 2	Stage V	28.6416	5.8212	11.664
	Stage IV	18.0144	6.5232	8.4456
	Stage III	16.9992	1.2744	7.7004
	Stage II	14.8176	1.6524	6.5232
	Stage I	14.8176	3.4344	7.9812
Can 3	Stage V	27.3672	4.8168	10.0548
	Stage IV	18.302	0.9072	7.3008
	Stage III	15.2604	2.4408	6.642
	Stage II	12.6468	2.8404	7.4196
	Stage I	11.4048	3.942	8.2836

Table 4: Average of "L", "a", and "b" Values of Experiment 4.

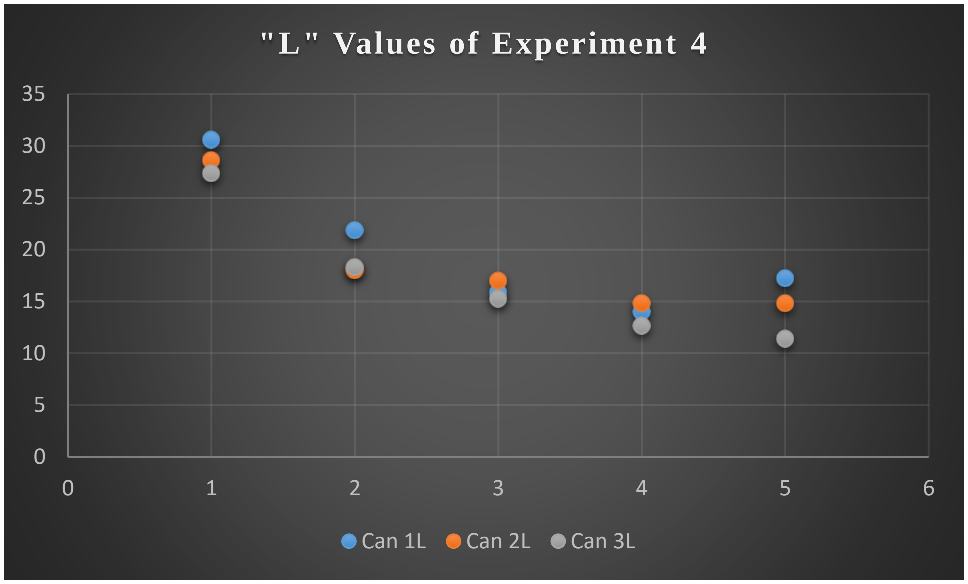

Figure 20: Average of "L" Values of Experiment 4.

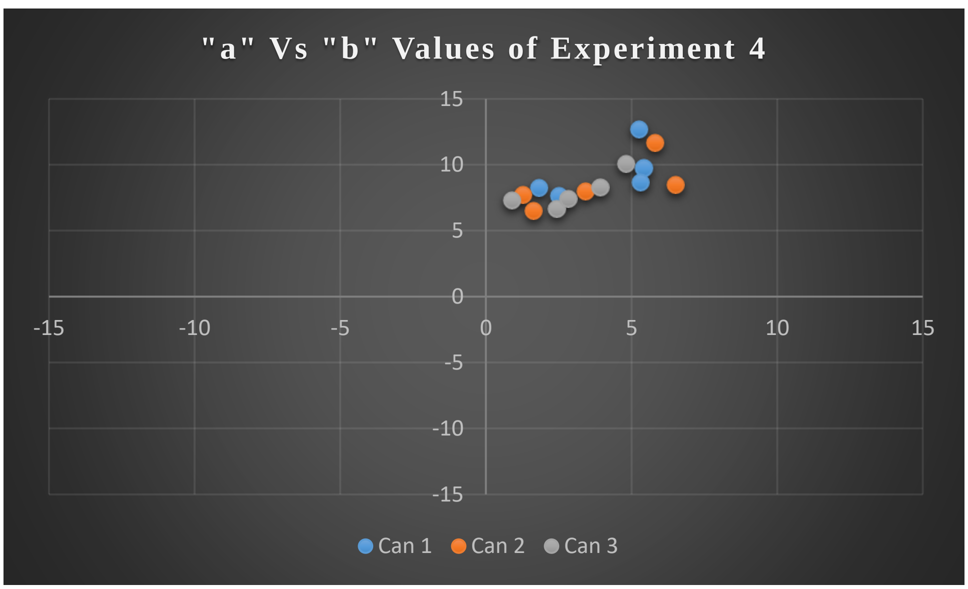

Figure 21: "a" Vs "b" Values of Experiment 4.

Soil Samples		L	a	b
Can 1	Stage V	27.7536	4.7824	11.5052
	Stage IV	19.8548	4.9294	8.8396
	Stage III	14.4256	1.225	7.4676
	Stage II	12.7008	2.096	6.9286
	Stage I	15.6408	4.8314	7.8792
Can 2	Stage V	25.9896	5.2822	10.584
	Stage IV	16.3464	5.9192	7.6636
	Stage III	15.4252	1.1564	6.9874
	Stage II	13.4456	1.4994	5.9192
	Stage I	13.4456	3.1164	7.2422
Can 3	Stage V	28.8332	4.3708	9.1238
	Stage IV	14.712	0.8232	6.6248
	Stage III	13.8474	2.2148	6.027
	Stage II	12.4758	2.5774	6.7326
	Stage I	11.3488	3.577	7.5166

Table 5: Average of "L", "a", and "b" Values of Experiment 5.

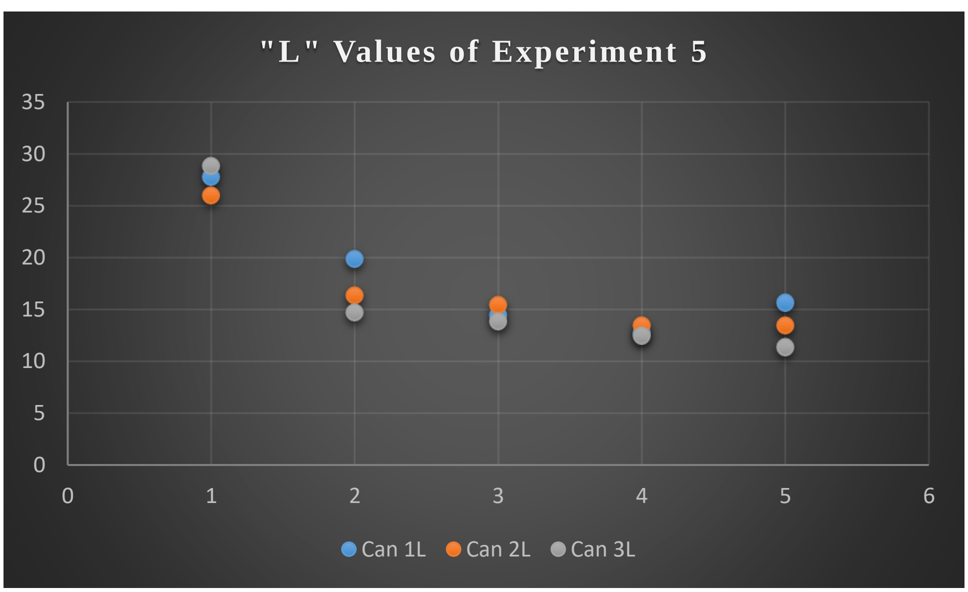

Figure 22: Average of "L" Values of Experiment 5.

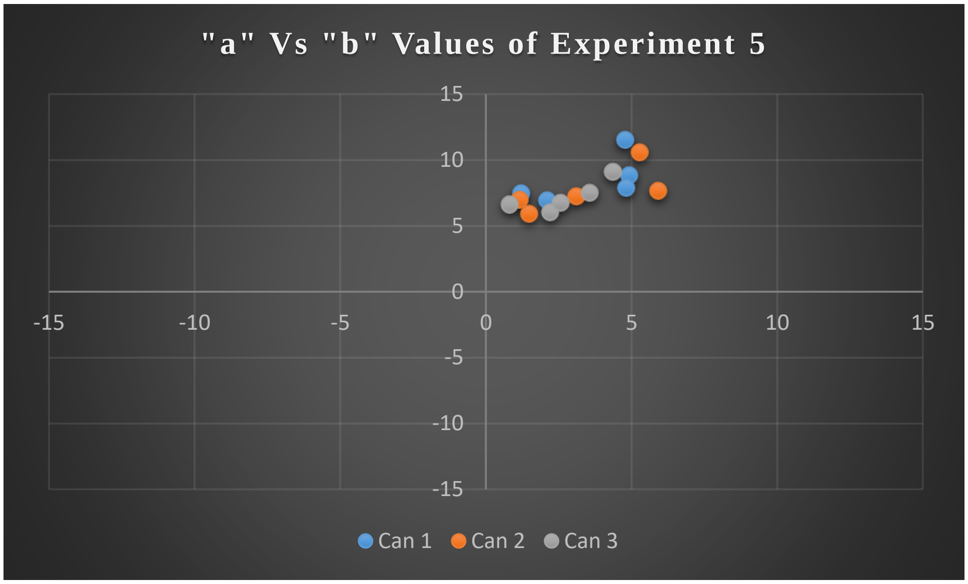

Figure 23: "a" Vs "b" Values of Experiment 5.

The evaluation of changes in soil color at various saturation stages in another color space was also taken into consideration with the RGB values.

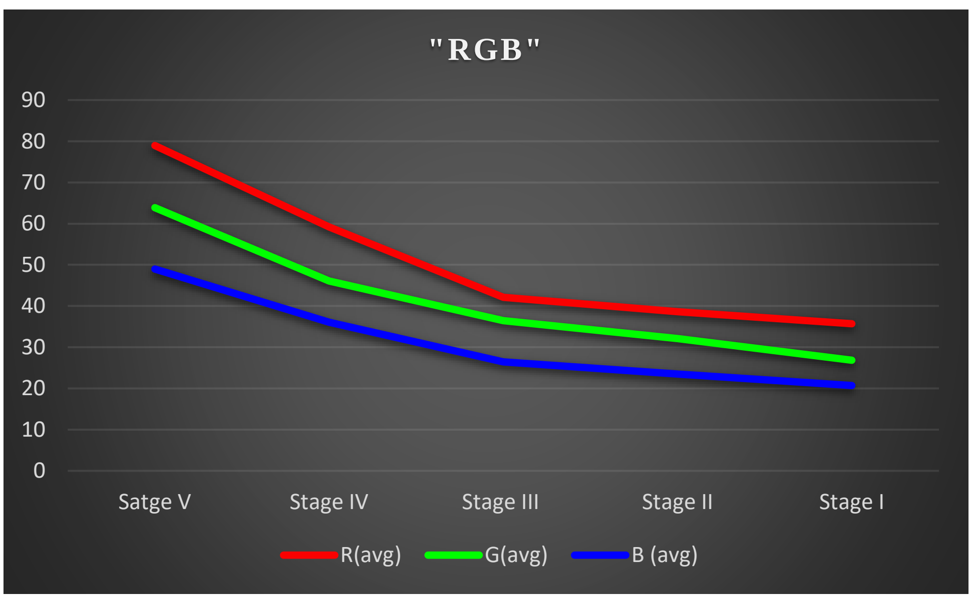

Figure 24: Average of "RGB".

The procedure of evaluating the values allow us to deduce that the "L" value, which stands for lightness and is the only significant component for determining the amount of moisture contained in the soil. Despite their correlation with the values of other samples obtained under the same conditions, the values of "a" and "b" revealed a large amount of variation at each stage of saturation. The fact that the fluctuations of "a" and "b" values at each stage do not follow any obvious pattern, it does not give us any reliable indication of the amount of moisture that is contained in the soil. The magnitude of the observed differences in RGB values does not meet the requirements for the building of a model that can accurately predict changes in soil moisture content using RGB values as the independent variable.

Therefore, the results of this research show that only the "L" values demonstrate changes that are statistically significant and strongly correlated in response to differences in the saturation stage of the soil.

5. CONCLUSION

The method used in this study expands the variety and usefulness of soil color obtained from digital scans, making it an approach that is simple, quick, and efficient for doing on-site research of land and crops. The color parameters “L”, “a”, and “b” that were obtained through the utilization of the Nix Pro equipment were chosen for the analysis because, in comparison to the results obtained from other parameters, they indicated a better association with one another at each stage. The procedure of evaluating the values enables us to get the conclusion that the "L" value, which stands for lightness and is the only component that plays a role in defining the soil's moisture content. The values of "a" and "b" revealed a significant amount of variability at each degree of saturation, despite the fact that they were associated with the values of other samples that had been taken under the exact same conditions. Due to the lack of identifiable patterns in the changes of "a" and "b" values at each step, the information regarding the moisture content of the soil cannot be relied upon.

The samples of soil were collected in a way that did not cause any disturbances, and the studies were carried out without subjecting the materials to any kind of pre-treatment. Therefore, it is likely that the samples contained additional substances, which might have resulted in discrepancies. It is advised that the indicated process for calibrating the soil color be supplemented by the collection of soil color data from a variety of soil samples located in a variety of places. This will allow for a more convincing conclusion to be drawn from the investigation. In addition, it is recommended to analyze whether shifts in the values of "L" reflect consistent patterns not only in the current case but also in subsequent cases. It is essential to carry out an investigation into the connection between the color of the soil and the amount of moisture it contains, making use of a greater variety of soil samples and working within the parameters of the framework presented in this study.

6. REFERENCES

Aitkenhead, M., Gaskin, G., Lafouge, N. and Hawes, C. (2017). PHYLIS: A Low-Cost Portable Visible Range Spectrometer for Soil and Plants. *Sensors*, 17(1), p.99. doi:https://doi.org/10.3390/s17010099.

Akalu, M.M. (2022). GIS-based land suitability assessment for surface irrigation: a case of Gilgel Gibe watershed, Jimma Zone, Ethiopia. *Arabian Journal of Geosciences*, 15(5). doi:https://doi.org/10.1007/s12517-022-09669-0.

Akbari, M., Gheysari, M., Mostafazadeh-Fard, B. and Shayannejad, M. (2018). Surface irrigation simulation-optimization model based on meta-heuristic algorithms. *Agricultural Water Management*, 201, pp.46–57. doi:https://doi.org/10.1016/j.agwat.2018.01.015.

Augusto, P., de, M., Madari, B.E. and Anselmo, E. de O. (2020). A computer-assisted soil texture analyzis using digitally scanned images. *Computers and Electronics in Agriculture*, 174, pp.105435–105435. doi:https://doi.org/10.1016/j.compag.2020.105435.

Ayushman Ramola, Amit Kumar Shakya and Dai Van Pham (2020). Study of statistical methods for texture analyzis and their modern evolutions. *Engineering reports*, 2(4). doi:https://doi.org/10.1002/eng2.12149.

Babalola, E.A., Asad, M. and Bais, A. (2023). Soil Surface Texture Classification Using RGB Images Acquired Under Uncontrolled Field Conditions. *IEEE Access*, 11, pp.67140–67155. doi:https://doi.org/10.1109/access.2023.3290907.

Barkunan, S.R., Bhanumathi, V. and Sethuram, J. (2019). Smart sensor for automatic drip irrigation system for paddy cultivation. *Computers & Electrical Engineering*, 73, pp.180–193. doi:https://doi.org/10.1016/j.compeleceng.2018.11.013.

Ben-Dor, E., Patkin, K., Banin, A. and Karnieli, A. (2002). Mapping of several soil properties using DAIS-7915 hyperspectral scanner data - a case study over clayey soils in Israel. *International Journal of Remote Sensing*, 23(6), pp.1043–1062. doi:https://doi.org/10.1080/01431160010006962.

Bi, Q., Qin, K., Li, Z., Zhang, H., Xu, K. and Xia, G.-S. (2020). A Multiple-Instance Densely-Connected ConvNet for Aerial Scene Classification. *IEEE Transactions on Image Processing*, 29, pp.4911–4926. doi:https://doi.org/10.1109/tip.2020.2975718.

Bi, Q., Qin, K., Zhang, H. and Xia, G.-S. (2021). Local Semantic Enhanced ConvNet for Aerial Scene Recognition. *IEEE Transactions on Image Processing*, 30, pp.6498–6511. doi:https://doi.org/10.1109/tip.2021.3092816.

Bortolini, L. and Tolomio, M. (2019). Influence of Irrigation Frequency on Radicchio (Cichorium Intybus L.) Yield. *Water*, 11(12), p.2473. doi:https://doi.org/10.3390/w11122473.

Çetin, O. and Kara, A. (2019). Assesment of water productivity using different drip irrigation systems for cotton. *Agricultural Water Management*, 223, p.105693. doi:https://doi.org/10.1016/j.agwat.2019.105693.

Chen, B., Shi, S., Sun, J., Chen, B., Guo, K., Du, L., Yang, J., Liu, F., Song, S. and Gong, W. (2021a). Using HSI Color Space to Improve the Multispectral Lidar Classification Error Caused by Measurement Geometry. *IEEE Transactions on Geoscience and Remote Sensing*, 59(4), pp.3567–3579. doi:https://doi.org/10.1109/tgrs.2020.3006577.

Chen, L., Chang, J., Wang, Y., Guo, A., Liu, Y., Wang, Q., Zhu, Y., Zhang, Y. and Xie, Z. (2021b). Disclosing the future food security risk of China based on crop production and water scarcity under diverse socioeconomic and climate scenarios. *Science of The Total Environment*, [online] 790, p.148110. doi:https://doi.org/10.1016/j.scitotenv.2021.148110.

Chen, R., Hong, L., Wang, J., Guo, X. and Song, Z. (2022). Comparisons of Spray Characteristics between Non-circular and Circular Nozzles with Rotating Sprinklers. *Applied Engineering in Agriculture*, 38(1), pp.61–75. doi:https://doi.org/10.13031/aea.14688.

Cheng, G., Han, J. and Lu, X. (2017). Remote Sensing Image Scene Classification: Benchmark and State of the Art. *Proceedings of the IEEE*, 105(10), pp.1865–1883. doi:https://doi.org/10.1109/jproc.2017.2675998.

Cheng, G., Li, Z., Yao, X., Guo, L. and Wei, Z. (2017). Remote Sensing Image Scene Classification Using Bag of Convolutional Features. *IEEE Geoscience and Remote Sensing*

Letters, 14(10), pp.1735–1739. doi:https://doi.org/10.1109/lgrs.2017.2731997.

Chung, S., Cho, K., Cho, J., Jung, K. and Yamakawa, T. (2012). Texture Classification Algorithm Using RGB Characteristics of Soil Images. *Journal of the Faculty of Agriculture, Kyushu University*, 57(2), pp.393–397. doi:https://doi.org/10.5109/25196.

Fan, Z., Herrick, J.E., Saltzman, R., Matteis, C., Yudina, A., Nocella, N., Crawford, E., Parker, R. and Van Zee, J. (2017). Measurement of Soil Color: A Comparison Between Smartphone Camera and the Munsell Color Charts. *Soil Science Society of America Journal*, 81(5), pp.1139–1146. doi:https://doi.org/10.2136/sssaj2017.01.0009.

Gamal, Y., Soltan, A., Said, L.A., Madian, A.H. and Radwan, A.G. (2023). Smart Irrigation Systems: Overview. *IEEE Access*, [online] pp.1–1. doi:https://doi.org/10.1109/ACCESS.2023.3251655.

Goap, A., Sharma, D., Shukla, A.K. and Rama Krishna, C. (2018). An IoT based smart irrigation management system using Machine learning and open source technologies. *Computers and Electronics in Agriculture*, 155, pp.41–49. doi:https://doi.org/10.1016/j.compag.2018.09.040.

Gunther Wyszecki and Stiles, W. (2000). Color Science: Concepts and Methods, Quantitative Data and Formulae, 2nd Edition. p.968.

Hamami, L. and Nassereddine, B. (2020). Application of wireless sensor networks in the field of irrigation: A review. *Computers and Electronics in Agriculture*, 179, p.105782. doi:https://doi.org/10.1016/j.compag.2020.105782.

Harmanny, K.S. and Malek, Ž. (2019). Adaptations in irrigated agriculture in the Mediterranean region: an overview and spatial analyzis of implemented strategies. *Regional Environmental Change*, 19(5), pp.1401–1416. doi:https://doi.org/10.1007/s10113-019-01494-8.

Huang, L., Zhao, W., Liew, A.W.-C. and You, Y. (2023a). An evidential combination method with multi-color spaces for remote sensing image scene classification. *Information Fusion*, [online] 93, pp.209–226. doi:https://doi.org/10.1016/j.inffus.2022.12.025.

Huang, L., Zhao, W., Liew, A.W.-C. and You, Y. (2023b). An evidential combination method with multi-color spaces for remote sensing image scene classification. *Information Fusion*, [online] 93, pp.209–226. doi:https://doi.org/10.1016/j.inffus.2022.12.025.

Jaconi, A., Vos, C. and Don, A. (2019). Near infrared spectroscopy as an easy and precise method to estimate soil texture. *Geoderma*, [online] 337, pp.906–913. doi:https://doi.org/10.1016/j.geoderma.2018.10.038.

Janaki Rama Suresh, G., Sreenivas, K. and Sivasamy, R. (2014). Hyperspectral analyzis of clay minerals. *ISPRS - International Archives of the Photogrammetry, Remote Sensing and Spatial Information Sciences*, XL-8, pp.443–446. doi:https://doi.org/10.5194/isprsarchives-xl-8-443-2014.

João Augusto Coblinski, Giasson, E., Alexandre, J., André Carnieletto Dotto, José Carlos Costa and Radim Vašát (2020). Prediction of soil texture classes through different wavelength regions of reflectance spectroscopy at various soil depths. 189, pp.104485–104485. doi:https://doi.org/10.1016/j.catena.2020.104485.

Khairul Huda Yusof, Aman, F., Ahmad Sukri Ahmad, M. Abdulrazaq, Mohammed, M.N., Mohamad and Yusuf, M. (2022). Determination of Soil Texture Using Image Processing Technique. doi:https://doi.org/10.1109/cspa55076.2022.9781996.

Kirchner, E., Koeckhoven, P. and Sivakumar, K. (2018). Improving Color Accuracy of Colorimetric Sensors. *Sensors*, 18(4), p.1252. doi:https://doi.org/10.3390/s18041252.

Kirchner, E., Koeckhoven, P. and Sivakumar, K. (2019). Predicting the performance of low-cost color instruments for color identification. *Journal of the Optical Society of America A*, 36(3), p.368. doi:https://doi.org/10.1364/josaa.36.000368.

Kirillova, N.P., Grauer-Gray, J., Hartemink, A.E., Sileova, T.M., Artemyeva, Z.S. and Burova, E.K. (2018). New perspectives to use Munsell color charts with electronic devices. *Computers and Electronics in Agriculture*, 155, pp.378–385. doi:https://doi.org/10.1016/j.compag.2018.10.028.

Lakhwani, K., Gianey, H., Agarwal, N. and Gupta, S. (2018). Development of IoT for Smart Agriculture a Review. *Advances in Intelligent Systems and Computing*, pp.425–432.

doi:https://doi.org/10.1007/978-981-13-2285-3_50.

Liu, Y., Liu, Y., Li, Y., Bian, P., Hu, Y., Zhang, J. and Shen, W. (2023). Effects of irrigation on the fate of microplastics in typical agricultural soil and freshwater environments in the upper irrigation area of the Yellow River. *Journal of Hazardous Materials*, [online] 447, p.130766. doi:https://doi.org/10.1016/j.jhazmat.2023.130766.

Mahmud, I. and Nafi, N.A. (2020). An approach of cost-effective automatic irrigation and soil testing system. *2020 Emerging Technology in Computing, Communication and Electronics (ETCCE)*. doi:https://doi.org/10.1109/etcce51779.2020.9350896.

Mauceri, A.A. and Banner, J.L. (2023). Resetting of soil compositions by irrigation in urban watersheds: Evidence from Sr isotope variations in Austin, TX. *Science of The Total Environment*, [online] p.166928. doi:https://doi.org/10.1016/j.scitotenv.2023.166928.

Morgan, C.L.S., Waiser, T.H., Brown, D.J. and Hallmark, C.T. (2009). Simulated in situ characterization of soil organic and inorganic carbon with visible near-infrared diffuse reflectance spectroscopy. *Geoderma*, 151(3-4), pp.249–256. doi:https://doi.org/10.1016/j.geoderma.2009.04.010.

Mouazen, A.M., Alexandridis, T., Buddenbaum, H., Cohen, Y., Moshou, D., Mulla, D., Nawar, S. and Sudduth, K.A. (2020). Monitoring. *Agricultural Internet of Things and Decision Support for Precision Smart Farming*, pp.35–138. doi:https://doi.org/10.1016/b978-0-12-818373-1.00002-0.

Muluneh, A., Tadesse, T. and Girma, R. (2022). Assessing potential land suitable for surface irrigation using GIS and AHP techniques in the Rift Valley Lakes Basin, Ethiopia. *Sustainable Water Resources Management*, 8(2). doi:https://doi.org/10.1007/s40899-022-00632-1.

Mwendwa, S. (2022). Revisiting soil texture analyzis: Practices towards a more accurate Bouyoucos method. *Heliyon*, [online] 8(5), p.e09395. doi:https://doi.org/10.1016/j.heliyon.2022.e09395.

Ng, W., Minasny, B., Mendes, W. de S. and Demattê, J.A.M. (2020). The influence of training sample size on the accuracy of deep learning models for the prediction of soil properties with near-infrared spectroscopy data. *SOIL*, 6(2), pp.565–578. doi:https://doi.org/10.5194/soil-6-565-2020.

Pramanik, M., Khanna, M., Singh, M., Singh, D.K., Sudhishri, S., Bhatia, A. and Ranjan, R. (2022). Automation of soil moisture sensor-based basin irrigation system. *Smart Agricultural Technology*, [online] 2, p.100032. doi:https://doi.org/10.1016/j.atech.2021.100032.

Ramos, T.B., Darouich, H., Oliveira, A.R., Farzamian, M., Monteiro, T., Castanheira, N., Paz, A., Alexandre, C., Gonçalves, M.C. and Pereira, L.S. (2023). Water use, soil water balance and soil salinization risks of Mediterranean tree orchards in southern Portugal under current climate variability: Issues for salinity control and irrigation management. *Agricultural Water Management*, [online] 283, p.108319. doi:https://doi.org/10.1016/j.agwat.2023.108319.

Sánchez-Marañón, M., Huertas, R. and Melgosa, M. (2005). Color variation in standard soil-color charts. *Soil Research*, 43(7), p.827. doi:https://doi.org/10.1071/sr04169.

Schmidt, S.A. and Ahn, C. (2019). A Comparative Review of Methods of Using Soil Colors and their Patterns for Wetland Ecology and Management. *Communications in Soil Science and Plant Analyzis*, 50(11), pp.1293–1309. doi:https://doi.org/10.1080/00103624.2019.1604737.

Shi, K., Lu, T., Zheng, W., Zhang, X. and Zhangzhong, L. (2022). A Review of the Category, Mechanism, and Controlling Methods of Chemical Clogging in Drip Irrigation System. *Agriculture*, [online] 12(2), p.202. doi:https://doi.org/10.3390/agriculture12020202.

Shivhare, S. and Cecil, K. (2021). *Automatic Soil Classification by using Gabor Wavelet & Support Vector Machine in Digital Image Processing*. [online] IEEE Xplore. doi:https://doi.org/10.1109/ICIRCA51532.2021.9544897.

Stiglitz, R., Mikhailova, E., Post, C., Schlautman, M. and Sharp, J. (2016). Evaluation of an inexpensive sensor to measure soil color. *Computers and Electronics in Agriculture*, [online] 121, pp.141–148. doi:https://doi.org/10.1016/j.compag.2015.11.014.

Tarik Mitran, T. Ravisankar, Fyzee, M.A., Suresh, J., G. Sujatha and K. Sreenivas (2015). Retrieval of soil physicochemical properties towards assessing salt-affected soils using Hyperspectral Data. *Geocarto International*, 30(6), pp.701–721.

doi:https://doi.org/10.1080/10106049.2014.985745.

Uddin, M. and Hassan, Md.R. (2022). A novel feature based algorithm for soil type classification. *Complex & Intelligent Systems*. doi:https://doi.org/10.1007/s40747-022-00682-0.

Vibhute, A.D. and Kale, K.V. (2023). Mapping several soil types using hyperspectral datasets and advanced machine learning methods. *Results in Optics*, 12, pp.100503–100503. doi:https://doi.org/10.1016/j.rio.2023.100503.

Viscarra Rossel, R.A., Minasny, B., Roudier, P. and McBratney, A.B. (2006). Color space models for soil science. *Geoderma*, 133(3-4), pp.320–337. doi:https://doi.org/10.1016/j.geoderma.2005.07.017.

Wang, J., Du, Y., Niu, W., Han, J., Li, Y. and Yang, P. (2022). Drip irrigation mode affects tomato yield by regulating root–soil–microbe interactions. *Agricultural Water Management*, 260, p.107188. doi:https://doi.org/10.1016/j.agwat.2021.107188.

Wang, L., Wu, W., Xiao, J., Huang, Q. and Hu, Y. (2021). Effects of different drip irrigation modes on water use efficiency of pear trees in Northern China. *Agricultural Water Management*, [online] 245, p.106660. doi:https://doi.org/10.1016/j.agwat.2020.106660.

Worqlul, A.W., Dile, Y.T., Jeong, J., Adimassu, Z., Lefore, N., Gerik, T., Srinivasan, R. and Clarke, N. (2019). Effect of climate change on land suitability for surface irrigation and irrigation potential of the shallow groundwater in Ghana. *Computers and Electronics in Agriculture*, 157, pp.110–125. doi:https://doi.org/10.1016/j.compag.2018.12.040.

Wu, Y., Mu, G., Qin, C., Miao, Q., Ma, W. and Zhang, X. (2020). Semi-Supervised Hyperspectral Image Classification via Spatial-Regulated Self-Training. *Remote Sensing*, 12(1), p.159. doi:https://doi.org/10.3390/rs12010159.

Wu, Y., Zhang, Y., Yuan, Y., Qin, A.K., Miao, Q. and Gong, M. (2022). Commonality Autoencoder: Learning Common Features for Change Detection From Heterogeneous Images. *IEEE transactions on neural networks and learning systems*, 33(9), pp.4257–4270. doi:https://doi.org/10.1109/tnnls.2021.3056238.

Xia, Q., Rufty, T. and Shi, W. (2020). Soil microbial diversity and composition: Links to soil texture and associated properties. *Soil Biology and Biochemistry*, 149, p.107953. doi:https://doi.org/10.1016/j.soilbio.2020.107953.

Yang, X., Shu, L., Chen, J., Ferrag, M.A., Wu, J., Nurellari, E. and Huang, K. (2021). A Survey on Smart Agriculture: Development Modes, Technologies, and Security and Privacy Challenges. *IEEE/CAA Journal of Automatica Sinica*, 8(2), pp.273–302. doi:https://doi.org/10.1109/jas.2020.1003536.

Yemane Weldewahid, Habtu, S., Taye, G., Kassa Teka and Tigist Araya Gessesse (2023). Effects of long-term irrigation practice on soil quality, organic carbon and total nitrogen stocks in the drylands of Ethiopia. *Journal of Arid Environments*, 214, pp.104982–104982. doi:https://doi.org/10.1016/j.jaridenv.2023.104982.

Yu, T., Fang, X., Yan, L., Zang, H., Zeng, Z. and Yang, Y. (2023). Irrigation rather than fertilization drives the abundance, community structure and assembly process of soil denitrifiers. *Agriculture, Ecosystems & Environment*, 357, pp.108688–108688. doi:https://doi.org/10.1016/j.agee.2023.108688.

Zong, R., Wang, Z., Li, W., Li, H. and Ayantobo, O.O. (2023). Effects of practicing long-term mulched drip irrigation on soil quality in Northwest China. *Science of The Total Environment*, 878, pp.163247–163247. doi:https://doi.org/10.1016/j.scitotenv.2023.163247.

Zou, Q., Ni, L., Zhang, T. and Wang, Q. (2015). Deep Learning Based Feature Selection for Remote Sensing Scene Classification. *IEEE Geoscience and Remote Sensing Letters*, 12(11), pp.2321–2325. doi:https://doi.org/10.1109/lgrs.2015.2475299.

7. DECLARATION

DECLARATION

the public access and authenticity of the thesis/dissertation/portfolio[1]

Student's name:	Mahmuda Rahman
Student's Neptun code:	VELW28
Title of thesis:	Master's Thesis
Year of publication:	2023
Name of the consultant's institute:	Institute of Agricultural and food Economics
Name of consultant's department:	Environmental Engineering

I declare that the final thesis/thesis/dissertation/portfolio submitted by me is an individual, original work of my own intellectual creation. I have clearly indicated the parts of my thesis or dissertation which I have taken from other authors' work and have included them in the bibliography.

If the above statement is untrue, I understand that I will be disqualified from the final examination by the final examination board and that I will have to take the final examination after writing a new thesis.

I do not allow editing of the submitted thesis, but I allow the viewing and printing, which is a PDF document.

I acknowledge that the use and exploitation of my thesis as an intellectual work is governed by the intellectual property management regulations of the Hungarian University of Agricultural and Life Sciences.

I acknowledge that the electronic version of my thesis will be uploaded to the library repository of the Hungarian University of Agricultural and Life Sciences. I acknowledge that the defended and

- not confidential thesis after the defense
- confidential thesis 5 years after the submission

will be available publicly and can be searched in the repository system of the University.

Date: 2023 year November month 11 day

Mahmuda

Student's signature

DECLARATION

I, András Barczi, dr. as a thesis insider consultant of Mahmuda Rahman (NEPTUN code: VELW28) declare that I have reviewed the final thesis and that I have informed the student of the requirements, legal and ethical rules for the correct handling of literary sources.

I recommend the final thesis to be defended in the final examination.

The thesis contains a state or official secret: yes **no**

Date: Gödöllő, 2023. year November month 11. day

ANDRÁS BARCZI

insider consultant